
Faculty of Science

Faculty Publications

This is a post-print version of the following article:

Multiple origins of obligate nematode and insect symbionts by a clade of bacteria closely related to plant pathogens

Vincent G. Martinson, Ryan M. R. Gawryluk, Brent E. Gowen, Caitlin I. Curtis, John Jaenike, & Steve J. Perlman

December 2020

The final publication is available at:

<https://doi.org/10.1073/pnas.2000860117>

Citation for this paper:

Martinson, V. G., Gawryluk, R. M. R., Gowen, B. E., Curits, C. I., Jaenike, J., & Perlman, S. J. (2020). Multiple origins of obligate nematode and insect symbionts by a clade of bacteria closely related to plant pathogens. *Proceedings of the National Academy of Sciences of the United States of America*, 117(50), 31979-31986. <https://doi.org/10.1073/pnas.2000860117>.

1 **Accepted Manuscript:**

2

3 Martinson VG, Gawryluk RMR, Gowen BE, Curtis CI, Jaenike J, Perlman SJ. 2020. Multiple
4 origins of obligate nematode and insect symbionts by a clade of bacteria closely related to plant
5 pathogens. *Proceedings of the National Academy of Sciences, USA*. 117, 31979-31986.
6 [doi/10.1073/pnas.2000860117](https://doi.org/10.1073/pnas.2000860117)

7

8 **Main Manuscript for**
9 Multiple origins of obligate nematode and insect symbionts by members of
10 a newly characterized bacterial clade
11
12

13 **Authors.**

14 Vincent G. Martinson^{1,2}, Ryan M. R. Gawryluk³, Brent E. Gowen³, Caitlin I. Curtis³, John Jaenike¹, Steve
15 J. Perlman³

16 ¹ Department of Biology, University of Rochester, Rochester, NY, USA, 14627

17 ² Department of Biology, University of New Mexico, Albuquerque, NM, USA, 87131

18 ³ Department of Biology, University of Victoria, Victoria, BC, Canada, V8W 3N5
19

20 **Corresponding author.**

21 Vincent G. Martinson, Department of Biology, MSC03 2020, 1 University of New Mexico, Albuquerque,
22 NM 87131-0001; Tel: 1-406-697-4660; Email: vmartinson@unm.edu
23

24 **ORCID.**

25 Vincent G. Martinson (ORCID: 0000-0001-5824-3548), Ryan M. R. Gawryluk (0000-0003-1251-882X),
26 Steve J. Perlman (0000-0002-9020-5506)
27

28 **Classification.**

29 Biological Sciences
30

31 **Keywords.**

32 *Howardula*, symbiosis, *Drosophila*, genome reduction, *Sodalis*
33

34 **Short Title.**

35 Widespread Symbiont of Nematodes and Insects
36

37 **Author Contributions.**

38 VGM, SJP, RMRG, and JJ designed and performed experiments and sequencing. BEG performed
39 electron microscopy. VGM performed analyses. CIC performed experiments. VGM and SJP wrote the
40 paper with input from all the authors.
41

42 **Competing Interests Statement.**

43 The authors declare no competing interest.
44

45 **This PDF file includes:**

46 Main Text	Supporting Information Appendix
47 Figures 1 to 4	Figures S1 to S7
48 Tables 1 to 2	Tables S1 to S2

49
50

51 **Abstract.**

52 Obligate symbioses involving intracellular bacteria have transformed eukaryotic life, from providing
53 aerobic respiration and photosynthesis, to enabling colonization of previously inaccessible niches, such
54 as feeding on xylem and phloem, and surviving in deep-sea hydrothermal vents. A major challenge in the
55 study of obligate symbioses is to understand how they arise. Because the best studied obligate
56 symbioses are ancient, it is especially challenging to identify early or intermediate stages. Here we report
57 the discovery of a nascent obligate symbiosis in *Howardula aoronymphium*, a well-studied nematode
58 parasite of *Drosophila* flies. We have found that *H. aoronymphium* and its sister species harbor a
59 maternally inherited intracellular bacterial symbiont. We never find the symbiont in nematode-free flies
60 and virtually all nematodes in the field and the lab are infected. Treating nematodes with antibiotics
61 causes a severe reduction in fly infection success. The association is recent, as more distantly related
62 insect-parasitic tylenchid nematodes do not host these endosymbionts. We also report that the
63 *Howardula* nematode symbiont is a member of a widespread monophyletic group of invertebrate host-
64 associated microbes that has independently given rise to at least four obligate symbioses, one in
65 nematodes and three in insects, and that is sister to *Pectobacterium*, a lineage of plant pathogenic
66 bacteria. Comparative genomic analysis of this group, which we name *Candidatus*
67 *Symbiopectobacterium*, shows signatures of genome erosion characteristic of early stages of symbiosis,
68 with the *Howardula* symbiont's genome containing over a thousand predicted pseudogenes, comprising a
69 third of its genome.

70

71 **Significance Statement.**

72 Obligate symbioses are intimate associations between species in which neither partner can live without
73 the other. It is challenging to study how obligate symbioses arise because they are often ancient and it is
74 difficult to uncover early or intermediate stages. We have discovered a nascent obligate symbiosis
75 involving *Howardula aoronymphium*, a well-studied nematode parasite of *Drosophila* flies, and a
76 bacterium related to *Pectobacterium*, a lineage of plant pathogens. Moreover, this nematode symbiont is
77 a member of a widespread group of invertebrate host-associated microbes that has independently given
78 rise to at least four obligate symbioses in nematodes and insects, making it an exciting model to study
79 transitions to obligate symbiosis.

80 **Introduction.**

81 Intimate symbioses involving intracellular bacteria have transformed eukaryotic life (1, 2), with
82 mitochondria and chloroplasts as canonical examples. More recent, yet still ancient, acquisitions of
83 obligate bacterial intracellular endosymbionts have enabled colonization and radiation by animals into
84 previously inaccessible niches, such as feeding on plant sap and animal blood (3), and surviving in deep-
85 sea hydrothermal vents (4). Among the most difficult questions to resolve in the study of obligate
86 symbiosis are how do obligate symbioses evolve, and where do obligate symbionts come from? This is
87 particularly challenging because most of the obligate symbioses that have been studied are ancient,
88 making it is extremely difficult to identify early or intermediate stages.

89
90 One of the most common ways to acquire an obligate symbiont is via symbiont replacement (5). As a
91 result of a lifestyle shaped by genetic drift, vertically transmitted obligate symbionts follow a syndrome of
92 accumulation of deleterious mutations, leading to genome degradation and reduction (6). A common
93 pattern is that they are replaced by other less-broken symbionts that may then renew the cycle of
94 genomic degradation (7). Here the symbiont, which is often descended from common facultative
95 symbionts or parasites (8, 9), is fitted into an established and well-functioning symbiosis (i.e. with a
96 'symbiont-experienced' host). For example, the symbiont *Sodalis* has independently given rise to
97 numerous obligate nutritional symbioses in blood-feeding flies and lice, sap-feeding mealybugs,
98 spittlebugs, hoppers, and grain-feeding weevils (9).

99
100 Less studied are young obligate symbioses in host lineages that did not already house obligate symbionts
101 (i.e. 'symbiont-naive' hosts') (10). Some of the best-known examples originate through host manipulation
102 by the symbiont via addiction or reproductive control. Addiction or dependence may be a common route
103 for obligate symbiosis (11), and one of the most famous examples occurred in the laboratory, on the
104 timescale of years, where strains of *Amoeba* evolved to become entirely dependent on intracellular
105 symbionts (12). Many maternally-inherited symbionts of terrestrial arthropods induce parthenogenetic (i.e.
106 all female) reproduction in their hosts (13); accumulation of deleterious mutations in genes required for
107 sexual reproduction will result in hosts that are unable to reproduce if cured of their symbiont (14).
108 However, despite advances in microbial surveys, there are still few examples of young obligate
109 symbioses that result in novel host functions. One intriguing example involves spheroid bodies, nitrogen-
110 fixing organelles found in rhopalodiacean diatoms, that originated from a single acquisition of a
111 cyanobacterial symbiont as recently as ~12 Mya (15, 16).

112
113 Here we report the discovery of a nascent obligate symbiosis in *Howardula aoronymphium*, a well-studied
114 nematode parasite of *Drosophila* (17), most recently in the context of a defensive symbiosis. A common
115 host species, *D. neotestacea*, harbors a strain of the facultative inherited symbiont *Spiroplasma* that
116 protects it against nematode-induced sterility (18). The protection provided by *Spiroplasma* is so strong
117 that symbiont-infected flies are spreading across N. America and replacing their uninfected counterparts
118 (19). Surprisingly, we have found that *H. aoronymphium* itself harbors an intracellular bacterial symbiont
119 that is related to *Pectobacterium*, a well-studied group of plant pathogens, often vectored by insects. We
120 also report that the nematode symbiont, which we name *Candidatus* *Symbiopectobacterium* (and
121 hereafter *Symbiopectobacterium*), is a member of a widespread lineage of invertebrate symbionts that
122 has independently given rise to at least four obligate symbioses, one in nematodes and three in insects,
123 representing an exciting new model for the study of obligate symbiosis.

124
125
126 **Results.**

127 *Virtually all H. aoronymphium in the field and lab host Symbiopectobacterium*

128 We surveyed wild-caught *Drosophila* spp. across North America and Europe, and over multiple
129 years, for the presence of *H. aoronymphium* and *Symbiopectobacterium*. Using specific primers for
130 *Symbiopectobacterium*, virtually all *Howardula*-infected flies were also positive for the symbiont (74 of 79,
131 Table 1; the 5 individuals that tested positive for *Howardula* but negative for *Symbiopectobacterium* may
132 have contained dead or dying nematodes). The symbiont was never amplified from *Drosophila* not
133 infected with *Howardula*. Our lab strain of *Howardula aoronymphium*, maintained in the lab for over ten
134 years, is also always infected with *Symbiopectobacterium*, and in a controlled laboratory infection of *D.*

135 *neotestacea* we confirmed the perfect association of *H. aoronymphium* and *Symbiopectobacterium*, i.e.
136 only nematode-infected flies are positive for the symbiont (Figure 1a).

137
138 *Symbiopectobacterium* is an intracellular inherited symbiont of *H. aoronymphium*

139 Within an adult fly host, a single adult parasitic female nematode, commonly referred to as a
140 motherworm at this stage, can produce around 500 larvae that fill her body until they rupture her
141 hypodermis, disseminate throughout the host fly hemocoel, and finally exit the fly through the intestinal or
142 genital tract (20). Using TEM and FISH microscopy, we observed pervasive bacterial infection in
143 nematode motherworms, juveniles developing within motherworms, and juveniles that have been
144 released from motherworms (Figure 1b-g; SI Appendix, Figure S1). In motherworms, this bacterium is
145 situated intracellularly within hypertrophied hypodermal cells, below the outer layer of microvilli, that
146 distinguish the parasitic female (SI Appendix, Figure S1). Within juveniles, bacteria are present in areas
147 consistent with hypodermal cells. 16S rRNA amplicon sequencing of *H. aoronymphium* was dominated by
148 *Symbiopectobacterium*, and there were no other potential symbiont sequences (SI Appendix, Figure S2).

149
150 Antibiotic treatment decreases *Howardula* parasitism success

151 We attempted to clear *Symbiopectobacterium* from *H. aoronymphium* by rearing nematodes on
152 their host *D. neotestacea* in media with the antibiotics ampicillin or rifampin. Adult flies were then
153 screened for nematodes and symbionts. The proportion of parasitized *D. neotestacea* was significantly
154 lower with ampicillin (0.085±0.03) and rifampin (no infection) compared to the control *H. aoronymphium*
155 exposure (0.25±0.9) (Control-Amp $\chi^2(1, N = 687) = 23.48, p < 0.0001$; Control-Rif $\chi^2(1, N = 469) = 45.74,$
156 $p < 0.0001$) (Figure 2a). Further, in a subset of flies that we dissected, *Symbiopectobacterium* was found
157 in all flies that contained motherworms (25/25), while visually non-parasitized flies were almost all
158 negative (41/45) (Figure 2b). Some visually non-parasitized flies were PCR positive for *H. aoronymphium*
159 but lacked *Symbiopectobacterium* (10/14), possibly indicating unsuccessful parasitism. Thus, we are at
160 present unable to generate symbiont-free nematodes.

161
162 *Symbiopectobacterium* is a common associate of a clade of *Drosophila*-parasitic nematodes

163 In order to determine if other insect-parasitic nematodes in the suborder Hexatyliina are
164 ancestrally associated with *Symbiopectobacterium*, we screened nematode species with a range of
165 primers designed to amplify *Symbiopectobacterium*. We detected *Symbiopectobacterium* in two close
166 relatives of *H. aoronymphium* that also parasitize *Drosophila* (21) - *H. neocosmis* and an unnamed
167 Japanese *Howardula* sp. (12/12 and 1/1 respectively) (Table 2). The *Symbiopectobacterium* *gyrA* gene
168 sequences amplified from these nematodes formed a strongly supported (100% bootstrap support)
169 monophyletic clade, sharing >99% nucleotide sequence identity (SI Appendix, Figure S3abc). In contrast,
170 *Symbiopectobacterium* was not found in two species of *Fergusobia* (0/6 individuals), the lineage that is
171 sister to *Drosophila*-parasitic *Howardula* (22), in *Parasitylenchus nearcticus*, a more distantly related
172 tylenchid parasite of *Drosophila* flies (21) (0/3 individuals), or in three unnamed nematodes that infect
173 sphaerocerid flies (0/13, 0/3, and 0/9), using a number of primers (*gyrA*, *groEL*, *purK* spacer, and 16S
174 rRNA genes) designed to target *Symbiopectobacterium*, as well as universal 16S rRNA primers (Table 2,
175 SI Appendix, Table S1, Figure S2, Figure S3c).

176
177 *Symbiopectobacterium* is an invertebrate-associated lineage allied with the plant-associated genus

178 *Pectobacterium*

179 A large number of gene sequences that had >97% sequence identity to the *Howardula* symbiont
180 16S rRNA gene were recovered from GenBank. Phylogenetic reconstruction revealed a monophyletic
181 clade closely related to the genera *Pectobacterium*, *Dickeya*, and *Brenneria* (SI Appendix, Figure S4).
182 This clade included several known intracellular symbionts, including in *Cimex* bed bugs (23), *Euscelidius*
183 leafhoppers (24), and *Chilacis* bulrush bugs (25); the remaining sequences were almost completely
184 observed in association with invertebrates (SI Appendix, Table S2). *Symbiopectobacterium* is most
185 commonly associated with insects from the order Hemiptera; however, these insects are taxonomically
186 diverse, sharing a most recent common ancestor nearly 300 Mya, and ecologically diverse with disparate
187 life history traits (e.g. blood-feeding, phloem-feeding, seed-feeding) (26).

188
189 Signatures of independent genome erosion across the *Symbiopectobacterium* clade

190 We sequenced the genomes of *Symbiopectobacterium* in nematodes and bulrush bugs, and
191 compared them with publicly available sequences of related symbionts in mealybugs (7), leafhoppers
192 (27), bed bugs (28), and parasitoid wasps (29), as well as free-living *Pectobacterium* (30). Regardless of
193 the three-fold size difference between the genomes of *Symbiopectobacterium* in nematodes (4.5 Mb) and
194 in bulrush bugs (1.5 Mb), both genomes harbored >90% of 203 single copy ortholog (SiCO)
195 gammaproteobacterial genes (31), indicating we captured nearly full chromosomes. Similarly, the
196 *Symbiopectobacterium* genomes recovered from the mealybug and parasitoid wasp genome projects
197 were nearly complete, containing 98% and 86% of the SiCO genes. Genomic fragments of the bed bug
198 and leafhopper symbionts were incomplete and lacked most of the SiCO genes, but could be positively
199 identified as members of the *Symbiopectobacterium* clade and were included in the genome tree (Figure
200 3, 4a).

201 Phylogenetic analysis of 203 single copy genes resulted in an overall branching pattern similar to
202 previous publications of Gammaproteobacteria (27, 32) and highly supported the *Symbiopectobacterium*
203 lineage within the plant-pathogenic 'soft rot Enterobacteriaceae' as the sister clade to the genera
204 *Pectobacterium* and *Brenneria* (Figure 3; SI Appendix, Figure S5). Regardless of sequence divergence,
205 species within the *Symbiopectobacterium* group shared large areas of gene order synteny with the
206 closely related *Pectobacterium carotovorum* genome. Alignment within syntenic regions revealed that,
207 although certain genomic rearrangements are shared, each genome has independent insertions,
208 deletions and mutations that have resulted in differential pseudogene formation (Figure 4bc).

209 Compared to their closest relative, *Pectobacterium carotovorum*, the *Symbiopectobacterium*
210 clade members had signatures of genome erosion often associated with the early stages of symbiosis,
211 including more pseudogenes, fewer tRNAs, shorter average CDS size, lower coding density, and
212 decreased genome size (Figure 4a). Despite their similarities, there is large variation among members of
213 *Symbiopectobacterium* in these same genomic traits, suggesting that they are at different stages in the
214 process of genomic reduction, which might be connected with the age of their association with their host
215 invertebrate. Using sequence divergence measurements (33), we estimate that *Symbiopectobacterium*
216 split from *Pectobacterium* 400-500 ky and the symbiosis events among *Symbiopectobacterium* species
217 occurred independently <100 ky (SI Appendix, Figure S6).

218 Along with genomic erosion, the metabolic potential of *Symbiopectobacterium* members has
219 changed greatly. Pseudogene formation or deletion has interrupted many of the amino acid and vitamin
220 synthesis pathways. While *Symbiopectobacterium* in nematodes has maintained many genes associated
221 with synthesis of amino acids and vitamins, chemotaxis, motility, and secretion systems, the bulrush bug
222 symbiont has lost the majority of functions, except for basic DNA replication and repair, and biosynthesis
223 of lysine and several vitamins.

224 Proposal of "Candidatus Symbiopectobacterium"

225 We propose the genus name "Candidatus Symbiopectobacterium" for the lineage of
226 Enterobacteriaceae that forms a monophyletic clade sister to *Pectobacterium* (SI Appendix, Figure S4),
227 and whose members are commonly found in association with diverse invertebrates, including intracellular
228 symbionts that are vertically transmitted within their host (i.e. symbionts of *Howardula aoronymphium*,
229 *Euscelidius variegatus*, *Cimex lectularius*, *Chilacis typhae*, and *Pseudococcus longispinus*). While the
230 16S rRNA gene in *Symbiopectobacterium* lacks sufficient genetic diversity to differentiate it from sister
231 genera at the historically used 95% similarity level, this lineage is clearly divergent in the phylogeny
232 produced with the genome-wide single-copy ortholog genes, which is mirrored in their ecological
233 associations. The symbionts of the bulrush bug and sycamore seed bug, *Chilacis typhae* and
234 *Belonochilus numenius*, respectively, have previously been named *Candidatus* Rohrkolberia, which refers
235 to the German word for bulrush (25, 34). It was recently pointed out that this name does not conform to
236 the current naming standards laid out in the International Code of Nomenclature of Prokaryotes (35, 36),
237 because the German word for bulrush is used instead of the Latin (Rule and Recommendation 6). Our
238 proposal of *Candidatus* Symbiopectobacterium would supersede the genus *Ca. Rohrkolberia*; this name
239 indicates both the widespread symbiotic nature of this lineage and its relatedness to *Pectobacterium*.

242 **Discussion**

243 We have discovered a nascent obligate symbiosis involving *Howardula aoronymphium*, a nematode
244 parasite of *Drosophila*, and a bacterium from a cryptic but widespread lineage of endosymbionts, allied
245

246 with *Pectobacterium*, and which we here name *Candidatus* *Symbiopectobacterium*. We present four
247 different lines of evidence supporting obligate symbiosis. First, there is almost perfect concordance
248 between *Symbiopectobacterium* and *H. aoronymphium* presence. We never detect symbionts in
249 nematode-free flies, and virtually all wild-caught flies that test positive for *H. aoronymphium* DNA are also
250 positive for *Symbiopectobacterium*. The very rare mismatches could be due to false negative PCR
251 amplification, perhaps due to low quality and/or low titer DNA, for example due to dead or dying
252 nematodes within a fly. Second, microscopy revealed intracellular bacterial infection, including inside
253 motherworms, juveniles developing inside motherworms, and shed juveniles. Third, closely related
254 symbionts were also detected in the sister species *H. neocosmis* and a Japanese *Howardula* sp. Finally,
255 treating nematodes with antibiotics caused a severe reduction in fly infection success, although we
256 cannot rule out the possibility that the antibiotic directly affected the nematode.

257
258 Only a handful of obligate symbioses involving nematodes and bacteria has been described, and these
259 include *Wolbachia* in some filarial nematodes (37), *Xiphinematobacter* and *Burkholderia* in some plant-
260 parasitic dagger nematodes (38, 39), *Photorhabdus* and *Xenorhabdus* in entomopathogenic nematodes
261 (40), and *Thiosymbion* sulfur-oxidizing ectosymbionts of marine stilbonematines (41). In contrast to many
262 nematode-bacterium associations, this symbiosis appears to be very young. We detected
263 *Symbiopectobacterium* only in the closely related *H. aoronymphium*, *H. neocosmis* and Japanese
264 *Howardula* sp., which represents just a sliver of the insect-parasitic, and *Drosophila*-parasitic, diversity
265 within the Hexatyliina (21, 42, 43). We were unable to amplify *Symbiopectobacterium* DNA in the related
266 nematodes *Fergusobia* sp., *Parasitylenchus nearcticus*, or three unnamed nematodes that infect
267 sphaeropterid flies. Nor did we find any evidence of bacterial endosymbiont infection in electron
268 microscopy studies of allied Hexatyliina nematodes, including *Deladenus*, *Thripinema*, and
269 *Contortylenchus* (44-46), and a very detailed and extensive study of *Howardula husseyi* (47) [note that
270 the genus *Howardula* is not monophyletic] (SI Appendix, Figure S3bc). As there is very little available
271 insect-parasitic nematode DNA sequence, it is difficult to provide an estimate for the age of the
272 *Symbiopectobacterium*-*Howardula* association. *Fergusobia* nematodes, the sister group of the *Howardula*
273 clade that hosts *Symbiopectobacterium*, are obligate mutualists of fergusoninid gall-making flies, and the
274 age of this family of flies has been estimated to be not more than 42 My (48, 49), providing a conservative
275 upper limit to the age of the symbiosis. Our sequence divergence measurements, however, suggest that
276 the symbiosis is much more recent, with *Symbiopectobacterium* splitting from *Pectobacterium* about a
277 half a million years ago.

278
279 *Symbiopectobacterium* is a surprisingly widespread lineage of symbionts, closely related to
280 *Pectobacterium*, *Dickeya*, and *Brenneria*, often referred to as 'soft rot Enterobacteriaceae' (SRE). These
281 SREs are common pathogens of plants that are often vectored by insects (50). The high sequence
282 similarity shared between *Symbiopectobacterium* and *Pectobacterium* (e.g. 16S rRNA gene) may explain
283 why this lineage has remained largely undetected despite the increase in amplicon surveys of
284 invertebrates. *Symbiopectobacterium* symbionts are diverse and include at least four independently
285 evolved obligate mutualistic symbioses – once in *Drosophila*-parasitic *Howardula*, and three times as a
286 nutritional symbiont in sap-feeding hemipteran insects, including a young symbiont replacement in
287 *Pseudococcus longispinus*, the long-tailed mealybug (7). They have also independently colonized the
288 lygaeoid seed bugs *Chilacis typhae*, the bulrush bug, and *Belonochilus numenius*, the sycamore seed
289 bug (25, 34). They are also common facultative symbionts of insects, including in *Cimex lectularius* bed
290 bugs (23), *Dipetalogaster maximus* and possibly related kissing bugs (51, 52), and *Euscelidius variegatus*
291 leafhoppers (24, 53). This latter symbiont, called BEV ('B'acterium of 'E'uscelidius 'v'ariegatus), was an
292 early model in insect symbiosis (53) that is noteworthy because it exhibits both transovarial and horizontal
293 transmission, and can be easily cultured on media outside the host. We also found some
294 *Symbiopectobacterium* sequences in GenBank that are not associated with invertebrate hosts, but
295 instead were identified in association with plants. These sequences may represent free-living
296 *Symbiopectobacterium* strains that have repeatedly forged symbioses with invertebrate hosts;
297 alternatively, new host-symbiont combinations may have become established via horizontal transmission
298 of facultative symbionts. *Symbiopectobacterium* is the fourth example of a lineage of symbionts that is
299 shared between insects and nematodes, joining *Wolbachia* (54), *Cardinium* (55), and *Burkholderia* (38,
300 56).

301

302 The evolution and distribution of *Symbiopectobacterium* is reminiscent of *Sodalis*, another widespread
303 lineage of mostly facultative insect symbionts that has repeatedly given rise to obligate nutritional
304 symbioses in sap and blood-feeding hemipterans and flies (9); acquisition of some *Sodalis* has been
305 estimated to have occurred very recently, ~30 kya (33). Like *Sodalis*, *Symbiopectobacterium* is an
306 exciting model for studying the evolution and dynamics of symbiosis, because it and its close relatives run
307 the gamut, from free-living, well-studied, genetically tractable pathogens (57, 58) to cultivable facultative
308 inherited symbionts, all the way to obligate symbionts. This diversity is also reflected in the dynamic
309 genome evolution of this lineage. Similar to *Sodalis* (33), the *Howardula* symbiont genome exhibits the
310 hallmark of recent symbiosis, as it is very large and full of pseudogenes.

311
312 So what is the role of *Symbiopectobacterium* in *Howardula*? There are a number of not mutually exclusive
313 possibilities. The symbiont may be boosting nematode fitness, for example, by aiding in evading the
314 *Drosophila* immune response, or providing a novel function, such as supplementing nutrition or
315 metabolism. One possibility is that the nematode symbiont supplements heme. While nematodes are the
316 only animals known to have lost the ability to synthesize heme (59), two lineages of animal-parasitic
317 nematodes have independently acquired the gene for ferrochelatase, the last step in the synthesis of
318 heme, via horizontal gene transfer from bacteria (60, 61); this enzyme, including conserved active sites, is
319 also encoded in the nematode *Symbiopectobacterium* genome. Alternatively, the symbiont may persist as
320 a result of addiction by the host (11), for example by producing a persistent toxin and its antidote, such
321 that symbiont removal is deleterious. The symbiont may also be providing an essential function that was
322 lost by the host. Comparing genomes of related nematodes with and without *Symbiopectobacterium*, as
323 well as transcriptome studies to uncover highly expressed symbiont genes, may provide some useful
324 clues. Interestingly, the role of the obligate *Wolbachia* symbiont of filarial nematodes is still unclear and
325 metabolic, defensive, and addictive processes have all been invoked (11, 62-64) particularly because a
326 number of species have lost *Wolbachia* without having gained new symbionts or genes (65, 66).

327
328

329 **Methods.**

330 PCR survey of *Symbiopectobacterium* in insect-parasitic nematodes

331 *Drosophila* flies collected at mushroom baits at sites in N. America, Europe, and Asia, were
332 individually subjected to DNA extraction and screened with specific primers for *Howardula* parasitism and
333 the presence of *Symbiopectobacterium*; additional samples were dissected to determine nematode
334 infection, followed by screening, which was done blind. Additionally, *Fergusonina* flies, that are obligately
335 associated with *Fergusobia* nematodes, were collected at eucalyptus trees and screened for
336 *Symbiopectobacterium*. Sphaerocerid flies were collected at mushroom baits and dissected for
337 nematodes, which were subsequently genotyped and screened for *Symbiopectobacterium*. 16S rRNA
338 amplicon sequencing was performed on *H. aoronymphium* and sphaerocerid nematode motherworms,
339 along with their uninfected fly hosts, *D. falleni* and *Spelobia* sp. Specific information about species
340 sampled, including dates, localities, primers and PCR conditions are available in the SI Appendix, SI
341 Materials and Methods.

342

343 Controlled *Howardula* and *Symbiopectobacterium* lab infection and qPCR

344 *Drosophila neotestacea* larvae were infected with *H. aoronymphium*. Upon emergence,
345 *Symbiopectobacterium* titer was quantified in two-day-old adult flies, using quantitative PCR. Specific
346 information about lab infection, and primers and qPCR conditions are available in the SI Appendix, SI
347 Materials and Methods.

348

349 Antibiotic exposure bioassay

350 To eliminate *Symbiopectobacterium* from *H. aoronymphium* and measure the subsequent
351 parasitism success, we exposed nematodes to ampicillin or rifampin and compared them to a control
352 group. Exposure lasted the entire parasitic life cycle. Briefly, free-living juvenile nematodes were allowed
353 to parasitize larval *D. neotestacea* and carry out development within fly pupae and adults as internal
354 parasites in vials with antibiotic impregnated food. One week post eclosion, adult flies were dissected to
355 ascertain nematode parasitism, and a subset were screened for *Symbiopectobacterium*. Each treatment
356 was repeated 4 times and the proportion of parasitism was assessed with a chi-squared test. Detailed

357 procedures for laboratory rearing and antibiotic treatment of *H. aoronymphium* are found in the SI
358 Appendix, SI Materials and Methods.

359

360 Microscopy to localize the symbiont of *Howardula*

361 Laboratory-reared *H. aoronymphium* were dissected from adult *Drosophila*, nematode samples
362 for TEM were prepared with Karnovsky's fixative before being embedded in Epon, whereas FISH samples
363 were fixed in Carnoy's solution for either TEM or FISH microscopy and probed with the general bacterial
364 target, Eub339. Detailed procedures for TEM and FISH are available in the SI Appendix, SI Materials and
365 Methods.

366

367 Sequencing, genome binning, and annotation of nematode and bulrush bug *Symbiopectobacterium*

368 DNA obtained from *H. aoronymphium*, dissected from lab-raised *Drosophila putrida*, was
369 sequenced with Illumina HiSeq technology and genome assembly was performed in UniCycler (67). The
370 *Symbiopectobacterium* genome was separated from the nematode and fly genomes using Blobtools (68)
371 and the de Bruijn graph visualization tool Bandage (69) (SI Appendix, Figure S7). Similar sequencing and
372 assembly methods were employed for the symbiont genome of the bulrush bug (*Chilacis typhae*). Gene
373 and metabolic pathways were annotated with Prokaryotic Genomes Annotation Pipeline (70, 71) and
374 KEGG Automatic Annotation Server (72) for each genome and gene synteny comparisons were made in
375 Geneious 11.1.5 (<https://www.geneious.com>) with Mauve (73). Detailed description of tissues, extraction,
376 sequence data, and assembly parameters used for genomic analyses are available in the SI Appendix, SI
377 Materials and Methods.

378

379 **Acknowledgements.**

380 We thank Sonja Scheffer for providing *Fergusobia* nematodes / *Fergusonina* flies; Evan Tandy for
381 maintaining *Drosophila* stocks; Alexandria Marshall and Finn Hamilton for help in the early stages of the
382 project; and Ben Parker and Ellen Martinson for constructive conversations. This study was supported by
383 National Science Foundation grant 1144581 to JJ and grants from the Natural Sciences and Engineering
384 Research Council of Canada (Discovery Grant Program) and the Swiss National Science Foundation
385 (Sinergia grant number CRSII3_154396) to SJP.

386

387 **Data Accessibility.**

388 Genomes are deposited in GenBank (SyHa, PRJNA415854; SyCt, PRJNA521717; SyPl, PRJNA510127;
389 SyDa, PRJNA510132; SyCl, PRJNA510131) and raw reads for SyHa and SyCt are available at the SRA
390 under the same bioprojects. Bacterial 16S rRNA (MK943676, MT859673, MT859692, MT859693), *gyrA*
391 (MN175990-MN175995, MT860065), and *groEL* (MT860063, MT860064) genes. Nematode 18S
392 (MN175314-MN175319, MT863735-MT863741) and CO1 (MN167829-MN167835) genes. Fly hosts CO1
393 (MT863696-MT863702). 16S rRNA amplicon dataset (PRJNA655365).

394

395

396 **References.**

- 397 1. N. A. Moran, Symbiosis. *Curr Biol* **16**, R866-R871 (2006).
- 398 2. N. A. Moran, Symbiosis as an adaptive process and source of phenotypic complexity. *Proc Natl*
399 *Acad Sci USA* **104**, 8627-8633 (2007).
- 400 3. N. Moran, J. P. McCutcheon, A. Nakabachi, Genomics and evolution of heritable bacterial
401 symbionts. *Annu Rev Genet* **42**, 165-190 (2008).
- 402 4. N. Dubilier, C. Bergin, C. Lott, Symbiotic diversity in marine animals: the art of harnessing
403 chemosynthesis. *Nat Rev Microbiol* **6**, 725-740 (2008).
- 404 5. S. Sudakaran, C. Kost, M. Kaltentpoth, Symbiont acquisition and replacement as a source of
405 ecological innovation. *Trends Microbiol* **25**, 375-390 (2017).
- 406 6. G. M. Bennett, N. A. Moran, Heritable symbiosis: the advantages and perils of an evolutionary
407 rabbit hole. *Proc Natl Acad Sci USA* **112**, 10169-10176 (2015).
- 408 7. F. Husnik, J. P. McCutcheon, Repeated replacement of an intrabacterial symbiont in the tripartite
409 nested mealybug symbiosis. *Proc Natl Acad Sci USA* **113**, E5416-E5424 (2016).
- 410 8. Y. Matsuura *et al.*, Recurrent symbiont recruitment from fungal parasites in cicadas. *Proc Natl*
411 *Acad Sci USA* **115**, E5970-E5979 (2018).

- 412 9. J. P. McCutcheon, B. M. Boyd, C. Dale, The life of an insect endosymbiont from the cradle to the
413 grave. *Curr Biol* **29**, R485-R495 (2019).
- 414 10. A. Y. Kostygov *et al.*, Novel trypanosomatid-bacterium association: evolution of endosymbiosis in
415 action. *mBio* **7** (2016).
- 416 11. W. Sullivan, *Wolbachia*, bottled water, and the dark side of symbiosis. *MBoC* **28**, 2343-2346
417 (2017).
- 418 12. K. W. Jeon, Development of cellular dependence on infective organisms: micrurgical studies in
419 amoebas. *Science* **176**, 1122-1123 (1972).
- 420 13. R. Stouthamer, "Wolbachia-induced parthenogenesis" in Influential Passengers: Inherited
421 Microorganisms and Arthropod Reproduction, S. L. O'Neill, A. A. Hoffmann, J. H. Werren, Eds.
422 (Oxford University Press, New York, 1997), pp. 102-124.
- 423 14. W. Ma, B. Pannebakker, L. Beukeboom, T. Schwander, L. Van de Zande, Genetics of decayed
424 sexual traits in a parasitoid wasp with endosymbiont-induced asexuality. *Heredity* **113**, 424-431
425 (2014).
- 426 15. T. Nakayama *et al.*, Spheroid bodies in rhopalodiacean diatoms were derived from a single
427 endosymbiotic cyanobacterium. *J Plant Res* **124**, 93-97 (2011).
- 428 16. T. Nakayama *et al.*, Complete genome of a nonphotosynthetic cyanobacterium in a diatom
429 reveals recent adaptations to an intracellular lifestyle. *Proc Natl Acad Sci USA* **111**, 11407-11412
430 (2014).
- 431 17. J. Jaenike, S. J. Perlman, Ecology and evolution of host-parasite associations: mycophagous
432 *Drosophila* and their parasitic nematodes. *Am Nat* **160**, S23-S39 (2002).
- 433 18. J. Jaenike, R. Unckless, S. N. Cockburn, L. M. Boelio, S. J. Perlman, Adaptation via symbiosis:
434 recent spread of a *Drosophila* defensive symbiont. *Science* **329**, 212-215 (2010).
- 435 19. S. N. Cockburn *et al.*, Dynamics of the continent-wide spread of a *Drosophila* defensive symbiont.
436 *Ecol Lett* **16**, 609-616 (2013).
- 437 20. H. E. Welch, Taxonomy, life cycle, development, and habits of two new species of
438 Allantonematidae (Nematoda) parasitic in drosophilid flies. *Parasitology* **49**, 83-103 (1959).
- 439 21. S. J. Perlman, G. S. Spicer, D. D. Shoemaker, J. Jaenike, Associations between mycophagous
440 *Drosophila* and their *Howardula* nematode parasites: a worldwide phylogenetic shuffle. *Mol Ecol*
441 **12**, 237-249 (2003).
- 442 22. W. Ye *et al.*, Molecular phylogenetics and the evolution of host plant associations in the
443 nematode genus *Fergusobia* (Tylenchida: Fergusobiinae). *Mol Phylogenet Evol* **45**, 123-141
444 (2007).
- 445 23. V. Hypša, S. Aksoy, Phylogenetic characterization of two transovarially transmitted
446 endosymbionts of the bedbug *Cimex lectularius* (Heteroptera: Cimicidae). *Insect Mol Biol* **6**, 301-
447 304 (1997).
- 448 24. B. C. Campbell, A. H. Purcell, Phylogenetic affiliation of BEV, a bacterial parasite of the
449 leafhopper *Euscelidius variegatus*, on the basis of 16S rDNA sequences. *Curr Microbiol* **26**, 37-41
450 (1993).
- 451 25. S. M. Kuechler, K. Dettner, S. Kehl, Characterization of an obligate intracellular bacterium in the
452 midgut epithelium of the bulrush bug *Chilacis typhae* (Heteroptera, Lygaeidae, Artheneinae). *Appl*
453 *Environ Microbiol* **77**, 2869-2876 (2011).
- 454 26. B. Misof *et al.*, Phylogenomics resolves the timing and pattern of insect evolution. *Science* **346**,
455 763-767 (2014).
- 456 27. P. H. Degnan *et al.*, Origin and examination of a leafhopper facultative endosymbiont. *Curr*
457 *Microbiol* **62**, 1565-1572 (2011).
- 458 28. J. B. Benoit *et al.*, Unique features of a global human ectoparasite identified through sequencing
459 of the bed bug genome. *Nat Comm* **7**, 10165 (2016).
- 460 29. E. S. Tvedte *et al.*, Genome of the parasitoid wasp *Diachasma alloeum*, an emerging model for
461 ecological speciation and transitions to asexual reproduction. *Genome Biol Evol* **11**, 2767-2773
462 (2019).
- 463 30. X. Li *et al.*, Comparative genomics of 84 *Pectobacterium* genomes reveals the variations related
464 to a pathogenic lifestyle. *BMC Genomics* **19**, 889 (2018).
- 465 31. E. Lerat, V. Daubin, N. A. Moran, From gene trees to organismal phylogeny in prokaryotes: the
466 case of the gamma-proteobacteria. *PLoS Biol* **1**, e19 (2003).

- 467 32. S. Denman *et al.*, *Brenneria goodwinii* sp. nov., associated with acute oak decline in the UK. *Int J*
468 *Syst Evol Microbiol* **62**, 2451-2456 (2012).
- 469 33. A. L. Clayton *et al.*, A novel human-infection-derived bacterium provides insights into the
470 evolutionary origins of mutualistic insect–bacterial symbioses. *PLoS Genet* **8**, e1002990 (2012).
- 471 34. S. M. Kuechler, P. Renz, K. Dettner, S. Kehl, Diversity of symbiotic organs and bacterial
472 endosymbionts of lygaeoid bugs of the families Blissidae and Lygaeidae (Hemiptera: Heteroptera:
473 Lygaeoidea). *Appl Environ Microbiol* **78**, 2648-2659 (2012).
- 474 35. A. Oren, A plea for linguistic accuracy—also for *Candidatus* taxa. *Int J Syst Evol Microbiol* **67**,
475 1085-1094 (2017).
- 476 36. C. T. Parker, B. J. Tindall, G. M. Garrity, International code of nomenclature of prokaryotes.
477 Prokaryotic code (2008 revision). *Int J Syst Evol Microbiol* **69**, S7-S111 (2015).
- 478 37. M. Sironi *et al.*, Molecular evidence for a close relative of the arthropod endosymbiont *Wolbachia*
479 in a filarial worm. *Mol Biochem Parasitol* **74**, 223-227 (1995).
- 480 38. J. E. Palomares-Rius, A. Archidona-Yuste, C. Cantalapiedra-Navarrete, P. Prieto, P. Castillo,
481 Molecular diversity of bacterial endosymbionts associated with dagger nematodes of the genus
482 *Xiphinema* (Nematoda: Longidoridae) reveals a high degree of phylogenetic congruence with
483 their host. *Mol Ecol* **25**, 6225-6247 (2016).
- 484 39. T. Vandekerckhove, A. Willems, M. Gillis, A. Coomans, Occurrence of novel verrucomicrobial
485 species, endosymbiotic and associated with parthenogenesis in *Xiphinema americanum*-group
486 species (Nematoda, Longidoridae). *Int J Syst Evol Microbiol* **50**, 2197-2205 (2000).
- 487 40. G. O. Poinar, G. M. Thomas, Significance of *Achromobacter nematophilus* Poinar and Thomas
488 (Achromobacteraceae: Eubacteriales) in the development of the nematode, DD-136
489 (*Neoplectana* sp. Steinernematidae). *Parasitology* **56**, 385-390 (1966).
- 490 41. M. F. Polz *et al.*, Phylogenetic analysis of a highly specific association between ectosymbiotic,
491 sulfur-oxidizing bacteria and a marine nematode. *Appl Environ Microbiol* **60**, 4461-4467 (1994).
- 492 42. V. N. Chizhov, N. N. Butorina, S. A. Subbotin, Entomoparasitic nematodes of the genus
493 *Skarbilovinema*: *S. laumondi* and *S. lyoni* (Nematoda: Tylenchida), parasites of the flies of the
494 family Syrphidae (Diptera), with phylogeny of the suborder Hexatyliina. *Russ J Nematol* **20**, 141-
495 155 (2012).
- 496 43. E. Koshel, V. Aleshin, G. Eroshenko, V. Kutyrev, Phylogenetic analysis of entomoparasitic
497 nematodes, potential control agents of flea populations in natural foci of plague. *BioMed Res Int*
498 <http://dx.doi.org/10.1155/2014/13521>, article 135218 (2014).
- 499 44. K. Sims, J. J. Becnel, J. Funderburk, The morphology and biology of the entomophilic *Thripinema*
500 *fuscum* (Tylenchida: Allantonematidae), and the histopathological effects of parasitism on the
501 host *Frankliniella fusca* (Thysanoptera: Thripidae). *J Nat Hist* **46**, 1111-1128 (2012).
- 502 45. S. A. Subbotin, V. N. Chizhov, Ultrastructure of the integument of parasitic females in
503 entomogenous tylenchids. II. *Howardula phyllotretae*, *Parasitylenchus dispar*, *Contortylenchus*
504 sp., and two allantonematid species. *Russ J Nematol* **4**, 131-138 (1996).
- 505 46. V. V. Yushin, H. Kosaka, M. Kusunoki, Spermatozoon ultrastructure in the sphaerularioidid
506 nematode *Contortylenchus genitalicola* (Tylenchomorpha: Sphaerularioidea). *Nematology* **8**, 191-
507 196 (2006).
- 508 47. I. L. Riding (1971) Studies on the biology and ultrastructure of nematodes parasitic in insects. in
509 *Department of Zoology & Applied Entomology* (Imperial College London, London, UK).
- 510 48. L. A. Nelson *et al.*, An emerging example of tritrophic coevolution between flies (Diptera:
511 Fergusoninidae) and nematodes (Nematoda: Neotylenchidae) on Myrtaceae host plants. *Biol J*
512 *Linnean Soc* **111**, 699-718 (2014).
- 513 49. B. M. Wiegmann *et al.*, Episodic radiations in the fly tree of life. *Proc Natl Acad Sci USA* **108**,
514 5690-5695 (2011).
- 515 50. S. Rossmann, M. W. Dees, J. Perminow, R. Meadow, M. B. Brurberg, Soft rot
516 Enterobacteriaceae are carried by a large range of insect species in potato fields. *Appl Environ*
517 *Microbiol* **84**, e00281-00218 (2018).
- 518 51. F. F. da Mota *et al.*, Cultivation-independent methods reveal differences among bacterial gut
519 microbiota in triatomine vectors of Chagas disease. *PLoS Neg Trop Dis* **6**, e1631 (2012).
- 520 52. S. Díaz, B. Villavicencio, N. Correia, J. Costa, K. L. Haag, Triatomine bugs, their microbiota and
521 *Trypanosoma cruzi*: asymmetric responses of bacteria to an infected blood meal. *Parasit Vectors*
522 **9**, 636 (2016).

- 523 53. A. H. Purcell, T. Steiner, F. Mégraud, J. Bové, In vitro isolation of a transovarially transmitted
524 bacterium from the leafhopper *Euscelidius variegatus* (Hemiptera: Cicadellidae). *J Invertebr*
525 *Pathol* **48**, 66-73 (1986).
- 526 54. M. Casiraghi *et al.*, Phylogeny of *Wolbachia pipientis* based on *gltA*, *groEL* and *ftsZ* gene
527 sequences: clustering of arthropod and nematode symbionts in the F supergroup, and evidence
528 for further diversity in the *Wolbachia* tree. *Microbiology* **151**, 4015-4022 (2005).
- 529 55. Y. Nakamura *et al.*, Prevalence of *Cardinium* bacteria in planthoppers and spider mites and
530 taxonomic revision of “*Candidatus Cardinium hertigii*” based on detection of a new *Cardinium*
531 group from biting midges. *Appl Environ Microbiol* **75**, 6757-6763 (2009).
- 532 56. K. Takeshita, Y. Kikuchi, *Riptortus pedestris* and *Burkholderia* symbiont: an ideal model system
533 for insect–microbe symbiotic associations. *Res Microbiol* **168**, 175-187 (2017).
- 534 57. J. Mansfield *et al.*, Top 10 plant pathogenic bacteria in molecular plant pathology. *Mol Plant*
535 *Pathol* **13**, 614-629 (2012).
- 536 58. I. K. Toth, K. S. Bell, M. C. Holeva, P. R. Birch, Soft rot erwiniae: from genes to genomes. *Mol*
537 *Plant Pathol* **4**, 17-30 (2003).
- 538 59. A. U. Rao, L. K. Carta, E. Lesuisse, I. Hamza, Lack of heme synthesis in a free-living eukaryote.
539 *Proc Natl Acad Sci USA* **102**, 4270-4275 (2005).
- 540 60. E. Nagayasu *et al.*, Identification of a bacteria-like ferrochelatase in *Strongyloides venezuelensis*,
541 an animal parasitic nematode. *PLoS ONE* **8**, e58458 (2013).
- 542 61. B. Wu *et al.*, Interdomain lateral gene transfer of an essential ferrochelatase gene in human
543 parasitic nematodes. *Proc Natl Acad Sci USA* **110**, 7748-7753 (2013).
- 544 62. A. C. Darby *et al.*, Analysis of gene expression from the *Wolbachia* genome of a filarial nematode
545 supports both metabolic and defensive roles within the symbiosis. *Genome Res* **22**, 2467-2477
546 (2012).
- 547 63. V. Foray, M. M. Pérez-Jiménez, N. Fattouh, F. Landmann, *Wolbachia* control stem cell behavior
548 and stimulate germline proliferation in filarial nematodes. *Dev Cell* **45**, 198-211.e193 (2018).
- 549 64. E. Lefoulon *et al.*, Breakdown of coevolution between symbiotic bacteria *Wolbachia* and their
550 filarial hosts. *PeerJ* **4**, e1840 (2016).
- 551 65. C. A. Desjardins *et al.*, Genomics of *Loa loa*, a *Wolbachia*-free filarial parasite of humans. *Nature*
552 *Genetics* **45**, 495-500 (2013).
- 553 66. E. Ferri *et al.*, New insights into the evolution of *Wolbachia* infections in filarial nematodes inferred
554 from a large range of screened species. *PLoS ONE* **6**, e20843 (2011).
- 555 67. R. R. Wick, L. M. Judd, C. L. Gorrie, K. E. Holt, Unicycler: resolving bacterial genome assemblies
556 from short and long sequencing reads. *PLoS Comput Biol* **13**, e1005595 (2017).
- 557 68. D. R. Laetsch, M. L. Blaxter, BlobTools: interrogation of genome assemblies. *F1000Res* **6**, 1287
558 (2017).
- 559 69. R. R. Wick, M. B. Schultz, J. Zobel, K. E. Holt, Bandage: interactive visualization of de novo
560 genome assemblies. *Bioinformatics* **31**, 3350-3352 (2015).
- 561 70. D. H. Haft *et al.*, RefSeq: an update on prokaryotic genome annotation and curation. *Nucleic*
562 *Acids Res* **46**, D851-D860 (2018).
- 563 71. T. Tatusova *et al.*, NCBI prokaryotic genome annotation pipeline. *Nucleic Acids Res* **44**, 6614-
564 6624 (2016).
- 565 72. Y. Moriya, M. Itoh, S. Okuda, A. C. Yoshizawa, M. Kanehisa, KAAS: an automatic genome
566 annotation and pathway reconstruction server. *Nucleic Acids Res* **35**, W182-W185 (2007).
- 567 73. A. E. Darling, B. Mau, N. T. Perna, progressiveMauve: multiple genome alignment with gene
568 gain, loss and rearrangement. *PLoS ONE* **5**, e11147 (2010).
- 569
570

571 **Figures Legends.**

572 Figure 1. *Symbiopectobacterium* is pervasive in *Howardula aoronymphium*. A. *Symbiopectobacterium*
573 relative abundance in *Drosophila neotestacea* not-parasitized (HA-) or parasitized (HA+) with *Howardula*
574 *aoronymphium* (qPCR measurements). B-G. Localization of bacteria within larval *Howardula* using FISH
575 microscopy; B. background autofluorescence, C. excitation of probe labeled bacteria. Localization of
576 *Symbiopectobacterium* to the *Howardula* hypodermis. Transmission electron microscopy image showing
577 bacterial cells visible in a *Howardula* young motherworm (D & E) and F1 instar larva (F & G) developing
578 within a *Drosophila neotestacea* individual.

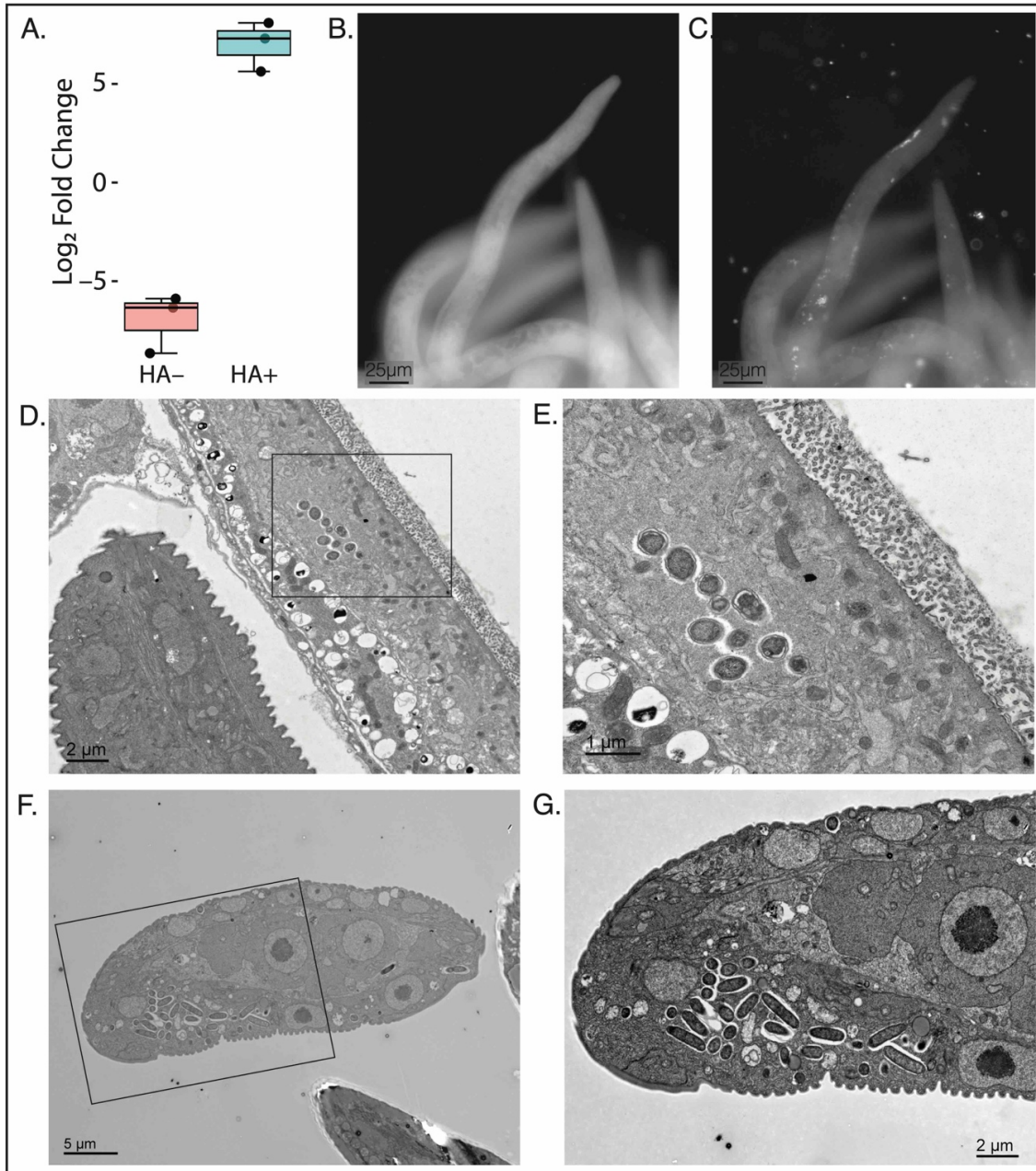
579
580 Figure 2. Experimental antibiotic exposure reduces or eliminates successful parasitism in *Howardula*
581 *aoronymphium*. A. Percent of adult *Drosophila* that were visually parasitized by *Howardula* with the
582 addition of different antibiotics (Control n=268, Ampicillin n=399, Rifampin n=181). B. PCR survey for
583 *Howardula* and *Symbiopectobacterium* in a subset of visually parasitized or non-parasitized *Drosophila*
584 individuals.

585
586 Figure 3. Phylogenetic tree of Gammaproteobacteria using the conserved set of 203 single copy
587 orthologous genes. The clade containing the *Howardula* symbiont, *Symbiopectobacterium* is sister to the
588 genera *Pectobacterium*, *Dickeya*, and *Brenneria* and other soft-rot Enterobacteriaceae. Taxonomic
589 classification of the host organism of each member of the putative symbiont clade. Phylogeny was
590 constructed with RAxML using 100 bootstrap replicates. The full phylogeny is available in SI Appendix,
591 Figure S5.

592
593 Figure 4. *Symbiopectobacterium* genomes compared to their closest relative, *Pectobacterium*
594 *carotovorum*. A. Comparison of genomic features. B. Example of conserved gene order across
595 *Symbiopectobacterium* species and *P. carotovorum*, highlighting the differential pseudogene events
596 across the symbiont clade. Red lines indicate contig boundaries. C. Analysis for central metabolic
597 pathways across *P. carotovorum* and the symbiont clade.

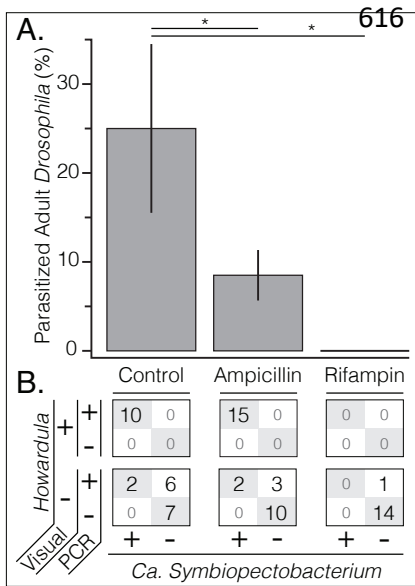
598
599 Table 1. PCR survey for *Symbiopectobacterium* in wild-caught *Drosophila neotestacea*.

600
601 Table 2. PCR survey for *Symbiopectobacterium* in wild-caught flies and parasitic nematodes.
602
603



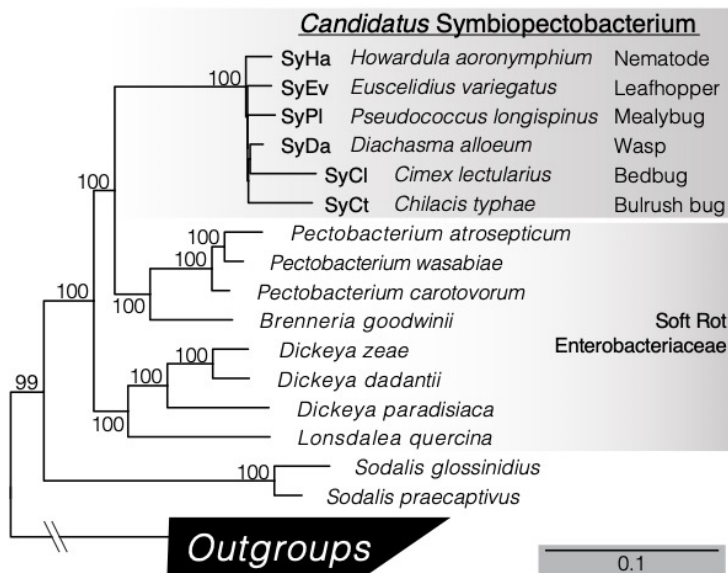
605
 606
 607
 608
 609
 610
 611
 612
 613
 614
 615

Figure 1. *Symbiopectobacterium* is pervasive in *Howardula aoronymphium*. A. *Symbiopectobacterium* relative abundance in *Drosophila neotestacea* not-parasitized (HA-) or parasitized (HA+) with *Howardula aoronymphium* (qPCR measurements). B-G. Localization of bacteria within larval *Howardula* using FISH microscopy; B. background autofluorescence, C. excitation of probe labeled bacteria. Localization of *Symbiopectobacterium* to the *Howardula* hypodermis. Transmission electron microscopy image showing bacterial cells visible in a *Howardula* young motherworm (D & E) and F1 instar larva (F & G) developing within a *Drosophila neotestacea* individual.



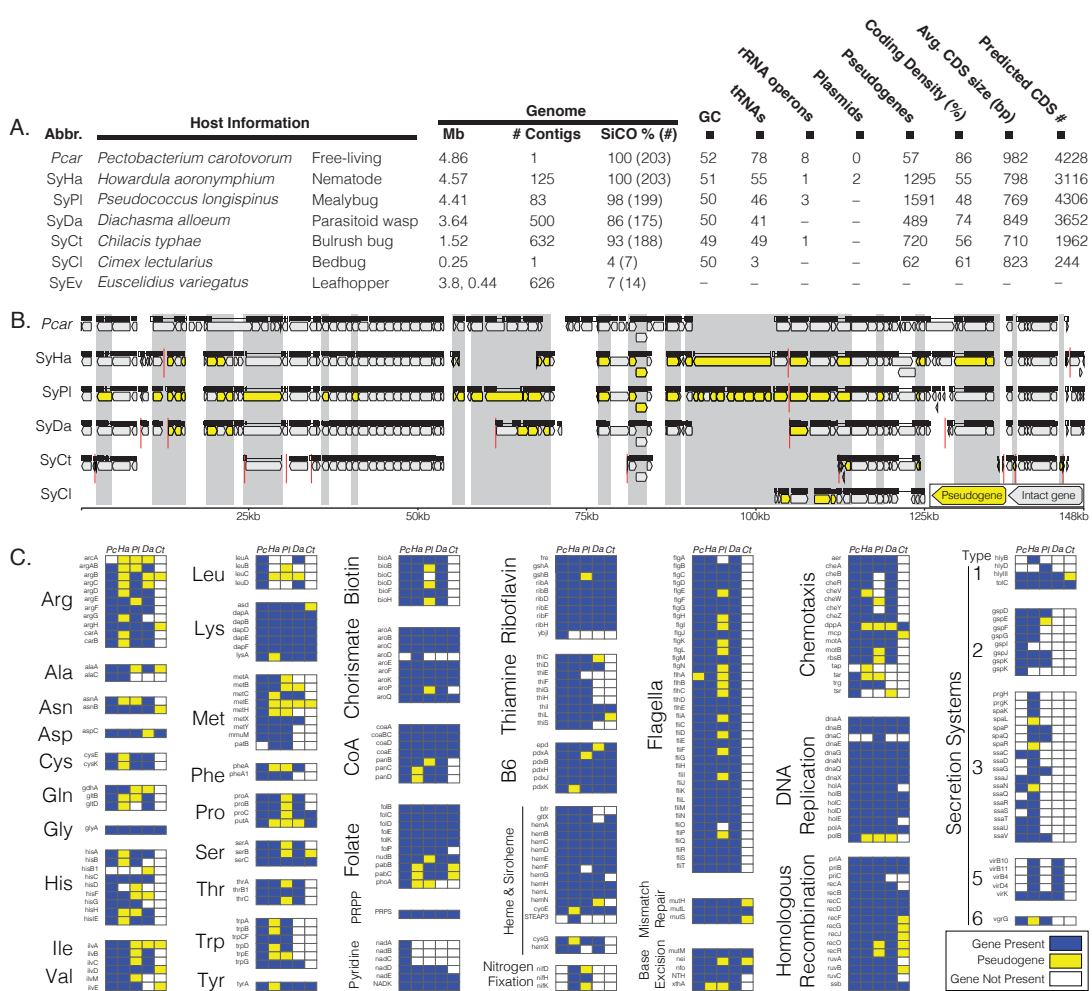
617
618
619
620
621
622
623
624
625

Figure 2. Experimental antibiotic exposure reduces or eliminates successful parasitism in *Howardula aoronymphium*. A. Percent of adult *Drosophila* that were visually parasitized by *Howardula* with the addition of different antibiotics (Control n=268, Ampicillin n=399, Rifampin n=181). B. PCR survey for *Howardula* and *Symbiopectobacterium* in a subset of visually parasitized or non-parasitized *Drosophila* individuals.



626
627
628
629
630
631
632
633
634
635

Figure 3. Phylogenetic tree of Gammaproteobacteria using the conserved set of 203 single copy orthologous genes. The clade containing the *Howardula* symbiont, *Symbiopectobacterium* is sister to the genera *Pectobacterium*, *Dickeya*, and *Brenneria* and other soft-rot Enterobacteriaceae. Taxonomic classification of the host organism of each member of the putative symbiont clade. Phylogeny was constructed with RAxML using 100 bootstrap replicates. The full phylogeny is available in SI Appendix, Figure S5.



636
637
638
639
640
641
642
643
644

Figure 4. *Symbiopectobacterium* genomes compared to their closest relative, *Pectobacterium carotovorum*. A. Comparison of genomic features. B. Example of conserved gene order across *Symbiopectobacterium* species and *P. carotovorum*, highlighting the differential pseudogene events across the symbiont clade. Red lines indicate contig boundaries. C. Analysis for central metabolic pathways across *P. carotovorum* and the symbiont clade.

645

Table 1. PCR survey for *Symbiopectobacterium* in wild-caught *Drosophila neotestacea*.

	<i>Howardula</i> +		<i>Howardula</i> –	
	<i>Sym.</i> +	<i>Sym.</i> –	<i>Sym.</i> +	<i>Sym.</i> –
2013	20	0	0	20
2014	8	5	0	27
2015	17	0	0	23
2020	29	0	0	55

Sym., *Symbiopectobacterium*; +, detected by PCR; –, not detected by PCR.

646

Table 2. PCR survey for *Symbiopectobacterium* in wild-caught flies and parasitic nematodes

	Nematode +		<i>Howardula</i> –	
	Sym. +	Sym. –	Sym. +	Sym. –
<i>Howardula aoronymphium</i> (England) (Host: <i>Drosophila</i>)	1	0	0	19
<i>Howardula aoronymphium</i> (Germany) (Host: <i>Drosophila</i>)	4	0	0	16
<i>Howardula</i> sp. B (Japan) (Host: <i>Drosophila</i>)	1	0	0	19
<i>Howardula neocosmis</i> (Host: <i>Drosophila</i>)	11	0	–	–
<i>Fergusobia</i> sp. (Host: <i>Fergusonina</i>)	0	6	–	–
<i>Parasitylenchus nearcticus</i> (Host: <i>Drosophila</i>)	0	3	–	–
<i>Spelobia</i> sphaerocerid parasite #1 (Host: <i>Spelobia</i>)	0	13	–	–
<i>Spelobia</i> sphaerocerid parasite #2 (Host: <i>Spelobia</i>)	0	3	–	–
<i>Spelobia</i> sphaerocerid parasite #3 (Host: <i>Spelobia</i>)	0	9	–	–

Sym., *Symbiopectobacterium*; +, detected by PCR; –, not detected by PCR.

647
648
649

1 Supporting Information for

2

3 **Multiple origins of obligate nematode and insect symbionts by members of a newly characterized**
4 **bacterial clade**

5

6 Vincent G. Martinson, Ryan M. R. Gawryluk, Brent E. Gowen, Caitlin I. Curtis, John Jaenike, Steve J.
7 Perlman

8

9 **Corresponding author.**

10 Vincent G. Martinson, Department of Biology, MSC03 2020, 1 University of New Mexico, Albuquerque,
11 NM 87131-0001; Tel: 1-406-697-4660; Email: vmartinson@unm.edu

12

13

14 **SI Materials and Methods.**

15
16 **Survey of *Candidatus* *Symbiopectobacterium* (hereafter *Symbiopectobacterium*) in insect-**
17 **parasitic nematodes.**

18 To determine how taxonomically and geographically widespread the association between
19 *Symbiopectobacterium* and insect-parasitic nematodes extends, we surveyed through a time series,
20 distant localities, and diverse nematode taxa.

21 Wild-collected *Drosophila neotestacea* were examined for *Howardula aoronymphium* parasitism
22 and the presence of *Symbiopectobacterium*. As part of a long-term survey of nematode prevalence, *D.*
23 *neotestacea* were collected monthly near Rochester, NY, DNA was extracted (Puregene kit, Qiagen,
24 Valencia, CA, USA), and individuals were screened with nematode-specific primers. We screened 20
25 putative *Howardula*-parasitized flies and 20 putative *Howardula*-unparasitized flies with nematode-specific
26 and *Symbiopectobacterium*-specific primers (Table S1), that had been collected consecutive Augusts
27 between 2013 and 2015. European flies are parasitized by *H. aoronymphium*, and therefore we screened
28 *Drosophila* collected at mushroom baits in 2009 from Southampton, United Kingdom and Munich,
29 Germany. In 2020, we collected wild *D. neotestacea* at mushroom baits in Victoria, BC, dissected them to
30 determine *Howardula aoronymphium* infection, and screened them, along with uninfected flies, for
31 *Symbiopectobacterium*; infection status was not known to the person performing the PCR screening.

32 We also surveyed the closest relatives of *H. aoronymphium*, two species that also parasitize
33 *Drosophila*: *H. neocosmis*, which is native to Florida and western N. America, and an unnamed species of
34 *Howardula* found in E. Asia. We screened 11 *D. munda* parasitized with *H. neocosmis* (Chiricahua
35 mountains, AZ, USA, 2008) and 20 *Drosophila* sp. collected in Sapporo, Japan (2009) for the closely
36 related unnamed *Howardula* species.

37 Outside of the *aoronymphium/neocosmis/unnamed* clade, the closest related genus is
38 *Fergusobia*. These nematodes are obligate symbionts with herbivorous flies (*Fergusonina* sp.), where
39 they are parasites of adults and live mutualistically in plant galls with fly larvae. We screened for
40 *Symbiopectobacterium* in three fly individuals of two species of *Fergusonina*. These specimens were
41 collected Australia from their native host trees: 1) Falls Creek Village, Victoria, *Eucalyptus pauciflora*, 24-
42 Sep-2007; 2) Kangaroo Island, South Australia, *Eucalyptus cosmophylla*, 19-Nov-2007. We also
43 screened the more distantly related *Parasitylenchus nearcticus*, a nematode that is native to N. America
44 and can also parasitize *D. neotestacea* (Vancouver, BC, 2002). Finally, we collected and dissected wild
45 sphaerocerid flies (mostly *Spelobia* sp.) at mushroom baits in Victoria, BC, in 2019 and 2020. We
46 amplified and sequenced nematode rRNA and attempted to amplify *Symbiopectobacterium* with a range
47 of primers. There were three tylenchid nematode species in these samples. *Fergusobia* and
48 *Parasitylenchus* were screened with purK spacer and gyrA primers for *Symbiopectobacterium* (Table S1).
49 Sphaerocerid parasites were screened with gyrA, groEL, 16S, and universal 16S primers.

50
51 **Nematode infection and *Symbiopectobacterium* titer.**

52 *Howardula aoronymphium*, *D. falleni*, and *D. neotestacea* were originally collected from
53 mushroom baits in West Hartford, CT, USA in 2006, and maintained in the laboratory on vials containing
54 mushrooms (*Agaricus bisporus*) and Carolina instant fly food; nematodes are maintained in *D. falleni* in
55 the lab. *Drosophila neotestacea* previously cured of *Wolbachia* and *Spiroplasma* infections were
56 incubated overnight on mushroom agar at 21°C. Eggs were collected in groups of 20 the subsequent
57 morning, and placed on mushroom wedges that were treated with either *Drosophila falleni* homogenate
58 containing approximately 400 *H. aoronymphium* infective juveniles in Ringer's solution (HA⁺ condition), or
59 an equivalent volume of homogenate from uninfected *D. falleni* (HA⁻ condition). A single mushroom
60 wedge was placed onto moistened cheesecloth in each vial.

61 Adult flies were collected immediately after eclosion and placed in solitary mushroom vials for two
62 days. Individual flies were homogenized in 50 µl of lysis buffer containing 100 mM Tris, pH 7.6, 100 mM
63 sodium chloride, 50 mM disodium EDTA, 1% w:v sodium dodecyl sulfate, and 0.1 mg/ml proteinase K
64 with 10-15 1 mm silica-zirconium beads in a Mini Beadbeater (BioSpec Products) for 10 s. Homogenates
65 were incubated at 65°C for one hour and extracted twice with 50 µl buffer-saturated phenol and 25 µl
66 chloroform. The final aqueous phase was combined with 5 µl of 3.3 M sodium acetate and precipitated
67 with 110 µl of ethanol. The pellet was washed twice with 200 µl of 75% ethanol and dissolved in 20 µl of
68 water.

69 Titer measurements for *Symbiopectobacterium* were carried out in a CFX96 Real-Time System
70 interfaced with CFX Manager 3.0 software using Applied Biosystems SYBR Select Master Mix (Applied
71 Biosystems, Carlsbad, CA, USA). The *D. neotestacea rpl32* gene was used as a positive control, and the
72 *rplQ* gene was used to measure *Symbiopectobacterium* titer. Three biological replicates were measured
73 for each condition (i.e., HA⁻ or HA⁺), and each primer set was measured in triplicate for each sample. Fold
74 changes in *Symbiopectobacterium* titer were calculated according to the Pfaffl method (1). Because *rplQ*
75 failed to amplify in all HA⁻ samples, we treated the Ct as 40. To compare HA⁺ and HA⁻ samples side-by-
76 side, we subtracted the Ct of each sample from that of the global mean. Primer efficiency (E) was
77 incorporated into the calculations as $1+E^{\Delta Ct}$.

78 79 **Effect of antibiotic on nematode parasitism.**

80 A population of *H. aoronymphium*, initially isolated from *D. neotestacea* collected at mushroom
81 baits (*Agaricus bisporus*) near Rochester, NY, was maintained in the laboratory using the host fly
82 *Drosophila putrida*. Briefly, parasitized adult *D. putrida* were homogenized in sterile H₂O to make a
83 suspension of free-living nematodes which were used to infect the next generation of *D. putrida* larvae.
84 Adult flies were allowed to oviposit for two days in standard *Drosophila* vials that contained Formula 4-24
85 Instant *Drosophila* Medium (Carolina Biological Supply Co, Burlington, NC, USA) hydrated with water and
86 a small mushroom slice (*Agaricus bisporus*). After oviposition, adults were removed from the vial and the
87 slurry containing juvenile nematodes was added. Nematodes were allowed to parasitize the *Drosophila*
88 larvae and resulting adult *D. putrida* were screened for nematode infection. *Howardula* used in this study
89 had been maintained in the laboratory for greater than five generations.

90 To determine the effect of antibiotics on nematode parasitism, lab-raised *D. neotestacea* were
91 infected with *H. aoronymphium* in the absence of antibiotics, with ampicillin, or with rifampicin. Nematodes
92 were exposed in vials that were prepared as above except the 4-24 media was hydrated with antibiotic
93 stocks to a final concentration of (100 µg/ml). Larvae were allowed to fully develop and adult *D.*
94 *neotestacea* were collected 6-7 days post eclosion to ensure that infecting-nematodes had the chance to
95 produce juveniles. Adult flies were dissected to observe nematodes and the proportion parasitized was
96 recorded. The parasitism experiment was performed in four replicate vials. To independently confirm the
97 presence of *H. aoronymphium* and *Symbiopectobacterium*, a subset of 10-15 flies that were visually
98 positive or negative were used for DNA extraction and screened with specific primers. Variation between
99 replicates was checked with a normal logistic fit test and significance was assessed in JMP using the chi-
100 square test.

101 102 **Microscopy to localize the symbiont of *Howardula*.**

103 Samples for TEM (a lab culture of *H. aoronymphium* adults and infectives, dissected from adult
104 *Drosophila falleni* and *D. neotestacea*) were double fixed and Epon embedded using standard TEM
105 methodology (2). After initial fixation in Karnovsky's fixative, the small samples were embedded within low
106 melt agarose (Sigma A9045) and the resulting blocks osmicated, dehydrated, infiltrated with Epon, and
107 the Epon polymerized. TEM sections were stained in uranyl acetate and lead citrate and viewed in a Jeol
108 JEM 1400 TEM at 80 kV. Images were captured using a Gatan SC-1000 digital camera.

109 The legs and head were removed from *H. aoronymphium*-parasitized *D. putrida* (from a lab
110 culture) to allow better penetration of the fixative and probes. Specimens were fixed with Carnoy's
111 solution overnight and rinsed with 100% EtOH using previously published methods (3). Fluorescent in situ
112 hybridization (FISH) microscopy was performed on as outlined in Martinson et al. 2012, on larval
113 nematodes that were released from the *D. putrida* body cavity following the final rinse step. The general
114 bacterial probe Eub339 was used to label all bacteria in larval nematodes (4).

115 116 **Genome of *Symbiopectobacterium* associated with the nematode, *Howardula aoronymphium*.**

117 A mix of juvenile and motherworm *H. aoronymphium* were dissected from infected *D. putrida* in
118 1x PBS buffer. The resulting nematodes were further rinsed twice with 1x PBS, for 30 sec in 2% bleach,
119 and again twice with 1x PBS. DNA was extracted with the DNeasy blood & tissue kit (Qiagen, Valencia,
120 CA, USA) and sequenced on the Illumina HiSeq2500 using 250 bp paired-end reads. Initial cleaning and
121 trimming of the data was performed with Trimmomatic-0.32 (5) using the commands
122 "SLIDINGWINDOW:4:20 TRAILING:13 LEADING:13 ILLUMINACLIP:adapters.fasta:2:30:10 MINLEN:15".
123 Because the sample contained a mix of DNA from the host (*Drosophila*), the parasite nematode
124 (*Howardula*), and microorganisms (including *Symbiopectobacterium* and any gut-associated microbiota),

125 an initial assembly was performed to partition contigs by taxonomic identity. Contigs assembled with
126 Metaspades (6) were classified by top blast hits to the GenBank nr database (accessed Feb 2016) and
127 visualized in plots based on length, GC content, and coverage using Bloobtools v1.0 (7). The fly and
128 nematode genomes were highly fragmented and could not be improved; however, we identified a putative
129 *Symbiopectobacterium* genome that comprised the long, high-coverage contigs and had top blast hits to
130 the genera *Pectobacterium* and *Brenneria* (Figure S7ab).

131 To improve the assembly and isolate this bacterial genome, a subset of the cleaned reads (24
132 million paired reads) were used for assembly with Unicycler v0.2.0 with the default settings (8). This
133 assembler utilizes SpADES (9) with multiple steps to iteratively improve assembly and to close circular
134 DNA (e.g. plasmids, bacterial chromosomes). Additionally, Unicycler outputs the de Bruijn graphs used to
135 create the assembly which preserve the tentative links between contigs that could not be integrated into
136 the final assembly because repeat regions create conflicting signal. After assembly, contigs were again
137 assigned a taxonomic identity by blast and Bloobtools. By loading each contigs taxonomic identity into the
138 genome assembly visualization tool Bandage (10) with the “csv” option and “Node labels: CSV data”, all
139 linked sets of contigs could be classified, binned as individual genomes, and analyzed separately (Figure
140 S7cd). The contigs identified as Proteobacteria were further error corrected and checked for overlaps with
141 the polish command in Unicycler. Contigs with fewer than 200 bp (256) were removed from the assembly,
142 after they were shown to not have sufficient sequence similarity to identify a top hit in GenBank or they
143 matched to insertion sequence (IS) families that were abundant in the genome. The final genomic contigs
144 were ordered relative to the closest genome sequence, *Pectobacterium carotovorum*, with Mauve (11)
145 using the progressiveMauve feature. Gene prediction and annotation (including pseudogene prediction)
146 was performed by the Prokaryotic Genomes Annotation Pipeline (PGAP) of NCBI (12, 13). To ensure that
147 the removal of short contigs (<200bp) had not artifactually led to the removal of genes in metabolic
148 pathway annotations, the top blast hit for each contig was identified.

149 **Genome of *Symbiopectobacterium* associated with the bulrush bug, *Chilacis typhae*.**

151 *Chilacis typhae* were collected from bulrushes (*Typha*) at Rithet’s Bog, Victoria, British Columbia,
152 Canada. Individual insects (~40 in total) were dissected with sterile pins, and the red ‘symbiont belt’ was
153 excised with a sterile razor blade. Symbiont belts were combined in 100 µl of cell lysis buffer containing
154 100 mM Tris pH 7.6, 100 mM sodium chloride, 50 mM disodium EDTA, 1% sodium dodecyl sulfate, and
155 0.1 mg/ml proteinase K, and manually disrupted with a plastic pestle. The homogenate was incubated
156 overnight at 65°C, and extracted twice with 100 µl buffer-saturated phenol and 50 µl chloroform,
157 precipitated with 100 µl of isopropanol, washed twice in 200 µl of 75% ethanol, and dissolved in TE buffer
158 (10 mM Tris, 1 mM disodium EDTA, pH 7.6). 0.3 µl of 100 mg/ml RNAse A (Qiagen) was added and the
159 solution was incubated for 20 minutes at room temperature. DNA was extracted, precipitated, washed,
160 and dissolved as described above. The presence of symbiont DNA was confirmed via Sanger sequencing
161 after PCR amplification of the 16S rRNA gene with primer pair Symbiopecto_16S F and R (Table S1).

162 Genomic DNA libraries were generated at the Genome Québec Innovation Centre using the
163 NEBNext Ultra II kit (New England Biolabs), and 125 bp paired-end reads were generated on an Illumina
164 HiSeq 2500 instrument from one third of a flow cell. The BBTools suite was used for quality control of
165 reads (<https://sourceforge.net/projects/bbmap/>). Raw sequence reads were trimmed for quality and
166 adaptor sequence with BBDuk, and reads ≥ 40 bp were retained. To remove reads from less abundant
167 symbiont belt bacteria prior to assembly, BBNorm was used to filter out kmers represented at a depth of
168 less than 200. SPAdes 3.10.1 (9) was used to assemble the genome, employing kmer values of 21, 33,
169 55, 77, and 99. Megablast (cite) was used to further decontaminate the genome assembly. Genomic
170 contigs for the symbiont chromosome were isolated with Bandage, <200 bp contigs removed, and
171 annotated with PGAP as performed for the *H. aoronymphium* symbiont.

172 **Genome comparisons.**

174 While querying GenBank with the *Howardula*-associated *Symbiopectobacterium*, several highly-
175 similar bacterial matches were identified within insect genome sequencing projects, including: the bed
176 bug (*Cimex lectularius*), the long-tailed mealybug (*Pseudococcus longispinus*), and a parasitoid wasp
177 (*Diachasma alloem*). Additionally, the incomplete genomic assembly of the symbiont “BEV” from a
178 leafhopper (*Euscelidius variegatus*) contained a few orthologous gene fragments that were found to have
179 high sequence similarity to *Symbiopectobacterium* (14). Sets of contigs, tentatively representing partial
180 bacterial genomes, were extracted from each of the insect genome projects, re-ordered, and annotated

181 with previously mentioned methods. The KEGG Automatic Annotation Server was used to find
182 orthologous genes and to evaluate the completeness of central metabolic pathways across the genus
183 *Symbiopectobacterium* and *P. carotovorum* (15). Gene order synteny was compared in Geneious 11.1.5
184 (<https://www.geneious.com>) using the multiple-genome alignment feature of the Mauve plugin (11).

185 186 **Phylogenetic reconstruction.**

187 The gyrase A gene (*gyrA*) of *Symbiopectobacterium* and CO1 and 18S rRNA genes from the
188 nematode and fly host were amplified from a subset of the *aoronymphium/neocosmis/unnamed*
189 specimens. Sanger sequencing was performed at Genewiz, Inc (South Plainfield, NJ, USA) or Sequetech
190 (Mountain View, CA, USA) and sequences were cleaned using Geneious. For each sequenced gene
191 (18S rRNA, CO1, *gyrA*) and for the bacterial 16S rRNA, closely related sequences were identified via
192 blast to GenBank and searching the Ribosomal Database Project (16). Sequences were aligned with
193 MUSCLE (17) in Geneious and phylogenies were built with RAxML (18) using 100 bootstrap replicates,
194 except for the 16S rRNA phylogeny that was built with Fasttree (19).

195 The genome phylogeny of Gammaproteobacteria was created with the 203 single-copy orthologs
196 (20). The gene set from *Escherichia coli K-12 substr. MG1655* was used to query each genome to find
197 top blast hits, each gene was individually aligned with MAFFT (21), and trimmed with gblocks (22, 23).
198 The resulting alignments were concatenated, and the full genome phylogeny was built with RAxML using
199 the GAMMA WAG model with 100 bootstrap replicates.

200 201 **Dating the *Symbiopectobacterium-Howardula* symbiosis.**

202 The age of the *Symbiopectobacterium* lineage was estimated by calculating the divergence time
203 of from *Pectobacterium* using sequence-based substitution rate measurements (24). Pairwise SiCO
204 genes were identified for each genome pair with the online tool OrthoVenn2 (25). Genes identified as
205 pseudogenes in the PGAP annotation pipeline (12) were excluded from further analysis to constrain the
206 analysis to only the most conserved regions of the genome. Amino acid sequence pairs for each SiCO
207 gene were individually aligned with MUSCLE (17) and codon-aligned nucleotide sequences were created
208 with pal2nal (26). Sequence changes were analyzed at only the 2nd codon positions because these are
209 the most functionally constrained sites. Substitutions at 2nd codon positions were calculated with custom
210 perl scripts incorporating codeml in PAML (27) and divergence times were estimated using the
211 measurement of 2.2×10^{-7} substitutions/site/year for the insect endosymbiont *Buchnera aphidicola* (28).

212 213 **16S rDNA amplicon sequencing.**

214 DNA was extracted and 16S rDNA amplicon sequencing was performed, for the following
215 samples: a) *Howardula aoronymphium* motherworms dissected out of *D. falleni*, from a nematode culture
216 maintained in the Perlman lab, and originally collected in West Hartford, CT, USA in 2006 (n=6), b)
217 uninfected *D. falleni* (n=4), c) sphaerocerid parasite species #3 motherworms, dissected from *Spelobia*
218 sp. flies collected at mushrooms baits in Victoria, BC, in 2020 (n=6), and d) uninfected *Spelobia* sp.
219 collected at the same baits (n=4).

220 Tissue was homogenized in 100 μ L of lysis buffer (100mM Tris-HCL, 100mM NaCl, 50mM
221 Na2EDTA and 1%SDS) and 0.5mg/mL Proteinase K (New England Biolabs Ltd.) in a Mini-Beadbeater.
222 Samples were incubated at 37°C for 20 minutes, followed by a de-activation of Proteinase K at 95°C for 5
223 minutes. A 1/10 volume of 3.3 M sodium acetate and 1 μ L of Glycogen (Thermoscientific) were added,
224 and samples were incubated at 65°C for one hour. DNA was isolated using the phenol-chloroform method
225 and precipitated with ethanol.

226 All DNA samples were normalized to a concentration of 20 ng/ μ L and submitted to GeneWiz
227 (South Plainfield, New Jersey) for construction of V3V4 hypervariable amplicon libraries, and 2 x 250 bp
228 paired-end sequencing using an Illumina MiSeq platform (*i.e.*, 16S-EZ service). Cutadapt v2.6 (50) was
229 used to remove 5' primers, and low-quality bases (< 20) from the 3' end of reads. All subsequent analyses
230 were carried out with R v.4.0.2 (R Core Team) within RStudio v1.2.5033 (RStudio Team). DADA2 v1.16
231 (51) was used for denoising, dereplication, merging, chimera detection, and inference of amplicon
232 sequence variants (ASVs). Briefly, forward and reverse reads were discarded if they were likely to contain
233 more than two erroneous base calls or were shorter than 200 bp; pseudo-pooling was used in ASV
234 inference; and read merging required \geq 20 bp of overlapping sequence. Taxonomic assignment of ASVs
235 was performed using Decipher v2.16.1 (52) based on the SILVA SSU r138 2019 dataset. Sampling depth
236 was normalized according to the variance stabilizing transformation using DESeq2 (53). Phyloseq v1.32.0

237 (54) was used to generate a proportion table containing sums of all ASVs within each bacterial family
238 contained in the dataset, and to subsequently filter the table to include only ASVs that make up > 5% of
239 any individual sample. A taxonomic boxplot was generated with ggplot2 v3.3.2 (55) to depict the
240 proportion of ASV counts from each bacterial family as a function of host (Figure S2).

241
242
243

SI References

- 244 1. M. W. Pfaffl, A new mathematical model for relative quantification in real-time RT-PCR. *Nucleic*
245 *Acids Res* **29**, e45 (2001).
- 246 2. M. Hayat, *Principles and techniques of electron microscopy: biological applications* (CRC Press,
247 Boca Raton, FL, USA, ed. 3rd, 1989).
- 248 3. R. Koga, T. Tsuchida, T. Fukatsu, Quenching autofluorescence of insect tissues for in situ
249 detection of endosymbionts. *Appl Entomol Zool* **44**, 281-291 (2009).
- 250 4. V. G. Martinson, J. Moy, N. A. Moran, Establishment of characteristic gut bacteria during
251 development of the honeybee worker. *Appl Environ Microbiol* **78**, 2830-2840 (2012).
- 252 5. A. M. Bolger, M. Lohse, B. Usadel, Trimmomatic: a flexible trimmer for Illumina sequence data.
253 *Bioinformatics* **30**, 2114-2120 (2014).
- 254 6. S. Nurk, D. Meleshko, A. Korobeynikov, P. A. Pevzner, metaSPAdes: a new versatile
255 metagenomic assembler. *Genome Res* **27**, 824-834 (2017).
- 256 7. D. R. Laetsch, M. L. Blaxter, BlobTools: interrogation of genome assemblies. *F1000Res* **6**, 1287
257 (2017).
- 258 8. R. R. Wick, L. M. Judd, C. L. Gorrie, K. E. Holt, Unicycler: resolving bacterial genome assemblies
259 from short and long sequencing reads. *PLoS Comput Biol* **13**, e1005595 (2017).
- 260 9. A. Bankevich *et al.*, SPAdes: a new genome assembly algorithm and its applications to single-cell
261 sequencing. *J Comput Biol* **19**, 455-477 (2012).
- 262 10. R. R. Wick, M. B. Schultz, J. Zobel, K. E. Holt, Bandage: interactive visualization of de novo
263 genome assemblies. *Bioinformatics* **31**, 3350-3352 (2015).
- 264 11. A. E. Darling, B. Mau, N. T. Perna, progressiveMauve: multiple genome alignment with gene
265 gain, loss and rearrangement. *PLoS ONE* **5**, e11147 (2010).
- 266 12. D. H. Haft *et al.*, RefSeq: an update on prokaryotic genome annotation and curation. *Nucleic*
267 *Acids Res* **46**, D851-D860 (2018).
- 268 13. T. Tatusova *et al.*, NCBI prokaryotic genome annotation pipeline. *Nucleic Acids Res* **44**, 6614-
269 6624 (2016).
- 270 14. P. H. Degnan *et al.*, Origin and examination of a leafhopper facultative endosymbiont. *Curr*
271 *Microbiol* **62**, 1565-1572 (2011).
- 272 15. Y. Moriya, M. Itoh, S. Okuda, A. C. Yoshizawa, M. Kanehisa, KAAS: an automatic genome
273 annotation and pathway reconstruction server. *Nucleic Acids Res* **35**, W182-W185 (2007).
- 274 16. J. R. Cole *et al.*, Ribosomal Database Project: data and tools for high throughput rRNA analysis.
275 *Nucleic Acids Res* **42**, D633-D642 (2014).
- 276 17. R. C. Edgar, MUSCLE: multiple sequence alignment with high accuracy and high throughput.
277 *Nucleic Acids Res* **32**, 1792-1797 (2004).
- 278 18. A. Stamatakis, RAxML-VI-HPC: maximum likelihood-based phylogenetic analyses with thousands
279 of taxa and mixed models. *Bioinformatics* **22**, 2688-2690 (2006).
- 280 19. M. N. Price, P. S. Dehal, A. P. Arkin, FastTree 2 - approximately maximum-likelihood trees for
281 large alignments. *PLoS ONE* **5**, e9490 (2010).
- 282 20. E. Lerat, V. Daubin, N. A. Moran, From gene trees to organismal phylogeny in prokaryotes: the
283 case of the gamma-proteobacteria. *PLoS Biol* **1**, e19 (2003).
- 284 21. K. Katoh, D. M. Standley, MAFFT Multiple Sequence Alignment Software Version 7:
285 Improvements in Performance and Usability. *Mol Biol Evol* **30**, 772-780 (2013).
- 286 22. J. Castresana, Selection of conserved blocks from multiple alignments for their use in
287 phylogenetic analysis. *Mol Biol Evol* **17**, 540-552 (2000).
- 288 23. G. Talavera, J. Castresana, Improvement of phylogenies after removing divergent and
289 ambiguously aligned blocks from protein sequence alignments. *Syst Biol* **56**, 564-577 (2007).
- 290 24. A. L. Clayton *et al.*, A novel human-infection-derived bacterium provides insights into the
291 evolutionary origins of mutualistic insect-bacterial symbioses. *PLoS Genet* **8**, e1002990 (2012).
- 292

- 293 25. L. Xu *et al.*, OrthoVenn2: a web server for whole-genome comparison and annotation of
294 orthologous clusters across multiple species. *Nucleic Acids Res* **47**, W52-W58 (2019).
- 295 26. M. Suyama, D. Torrents, P. Bork, PAL2NAL: robust conversion of protein sequence alignments
296 into the corresponding codon alignments. *Nucleic Acids Res* **34**, W609-W612 (2006).
- 297 27. Z. Yang, PAML 4: phylogenetic analysis by maximum likelihood. *Mol Biol Evol* **24**, 1586-1591
298 (2007).
- 299 28. N. A. Moran, H. J. McLaughlin, R. Sorek, The dynamics and time scale of ongoing genomic
300 erosion in symbiotic bacteria. *Science* **323**, 379-382 (2009).
- 301 29. B. C. Campbell, A. H. Purcell, Phylogenetic affiliation of BEV, a bacterial parasite of the
302 leafhopper *Euscelidius variegatus*, on the basis of 16S rDNA sequences. *Curr Microbiol* **26**, 37-41
303 (1993).
- 304 30. F. F. da Mota *et al.*, Cultivation-independent methods reveal differences among bacterial gut
305 microbiota in triatomine vectors of Chagas disease. *PLoS Neg Trop Dis* **6**, e1631 (2012).
- 306 31. S. Díaz, B. Villavicencio, N. Correia, J. Costa, K. L. Haag, Triatomine bugs, their microbiota and
307 *Trypanosoma cruzi*: asymmetric responses of bacteria to an infected blood meal. *Parasit Vectors*
308 **9**, 636 (2016).
- 309 32. O. Duron *et al.*, The diversity of reproductive parasites among arthropods: *Wolbachia* do not walk
310 alone. *BMC Biol.* **6**, 12 (2008).
- 311 33. T. Hosokawa, R. Koga, Y. Kikuchi, X.-Y. Meng, T. Fukatsu, *Wolbachia* as a bacteriocyte-
312 associated nutritional mutualist. *Proc Natl Acad Sci USA* **107**, 769-774 (2010).
- 313 34. F. Husnik, J. P. McCutcheon, Repeated replacement of an intrabacterial symbiont in the tripartite
314 nested mealybug symbiosis. *Proc Natl Acad Sci USA* **113**, E5416-E5424 (2016).
- 315 35. R. Koga, N. A. Moran, Swapping symbionts in spittlebugs: evolutionary replacement of a reduced
316 genome symbiont. *ISME J* **8**, 1237-1246 (2014).
- 317 36. S. M. Kuechler, P. Renz, K. Dettner, S. Kehl, Diversity of symbiotic organs and bacterial
318 endosymbionts of lygaeoid bugs of the families Blissidae and Lygaeidae (Hemiptera: Heteroptera:
319 Lygaeoidea). *Appl Environ Microbiol* **78**, 2648-2659 (2012).
- 320 37. Y. Matsuura *et al.*, Evolution of symbiotic organs and endosymbionts in lygaeid stinkbugs. *ISME J*
321 **6**, 397-409 (2012).
- 322 38. A. R. Pitman, P. J. Wright, M. D. Galbraith, S. A. Harrow, Biochemical and genetic diversity of
323 pectolytic enterobacteria causing soft rot disease of potatoes in New Zealand. *Australasian Plant*
324 *Pathology* **37**, 559-568 (2008).
- 325 39. H. Salmonová, J. Killer, V. Bunešová, M. Geigerová, E. Vlková, Cultivable bacteria from
326 *Pectinatella magnifica* and the surrounding water in South Bohemia indicate potential new
327 Gammaproteobacterial, Betaproteobacterial and Firmicutes taxa. *FEMS Microbiol Lett* **365**
328 (2018).
- 329 40. N. Someya, Y. Ohdaira Kobayashi, S. Tsuda, S. Ikeda, Molecular characterization of the bacterial
330 community in a potato phytosphere. *Microbes and Environments* **28**, 295-305 (2013).
- 331 41. E. Yashiro, P. S. McManus, Effect of streptomycin treatment on bacterial community structure in
332 the apple phyllosphere. *PLoS ONE* **7**, e37131 (2012).
- 333 42. M. J. Ballinger, R. M. R. Gawryluk, S. J. Perlman, Toxin and genome evolution in a *Drosophila*
334 defensive symbiosis. *Genome Biol Evol* **11**, 253-262 (2018).
- 335 43. R. M. Floyd, A. D. Rogers, P. J. D. Lamshead, C. R. Smith, Nematode-specific PCR primers for
336 the 18S small subunit rRNA gene. *Molecular Ecology Notes* **5**, 611-612 (2005).
- 337 44. O. Folmer, M. Black, W. Hoeh, R. Lutz, R. Vrijenhoek, DNA primers for amplification of
338 mitochondrial cytochrome c oxidase subunit I from diverse metazoan invertebrates. *Mol Mar Biol*
339 *Biotechnol* **3**, 294-299 (1994).
- 340 45. J. Jaenike, T. D. Brekke, Defensive endosymbionts: a cryptic trophic level in community ecology.
341 *Ecol Lett* **14**, 150-155 (2011).
- 342 46. J. R. Marchesi *et al.*, Design and evaluation of useful bacterium-specific PCR primers that amplify
343 genes coding for bacterial 16S rRNA. *Appl Environ Microbiol* **64**, 795-799 (1998).
- 344 47. V. G. Martinson *et al.*, A simple and distinctive microbiota associated with honey bees and
345 bumble bees. *Mol Ecol* **20**, 619-628 (2011).
- 346 48. J. P. Sandström, J. A. Russell, J. P. White, N. A. Moran, Independent origins and horizontal
347 transfer of bacterial symbionts of aphids. *Mol Ecol* **10**, 217-228 (2001).

- 348 49. L. Iasur-Kruh *et al.*, Bacterial associates of *Hyalesthes obsoletus* (Hemiptera: Cixiidae), the insect
349 vector of bois noir disease, with a focus on cultivable bacteria. *Res Microbiol* **168**, 94-101 (2017).
350
351
352

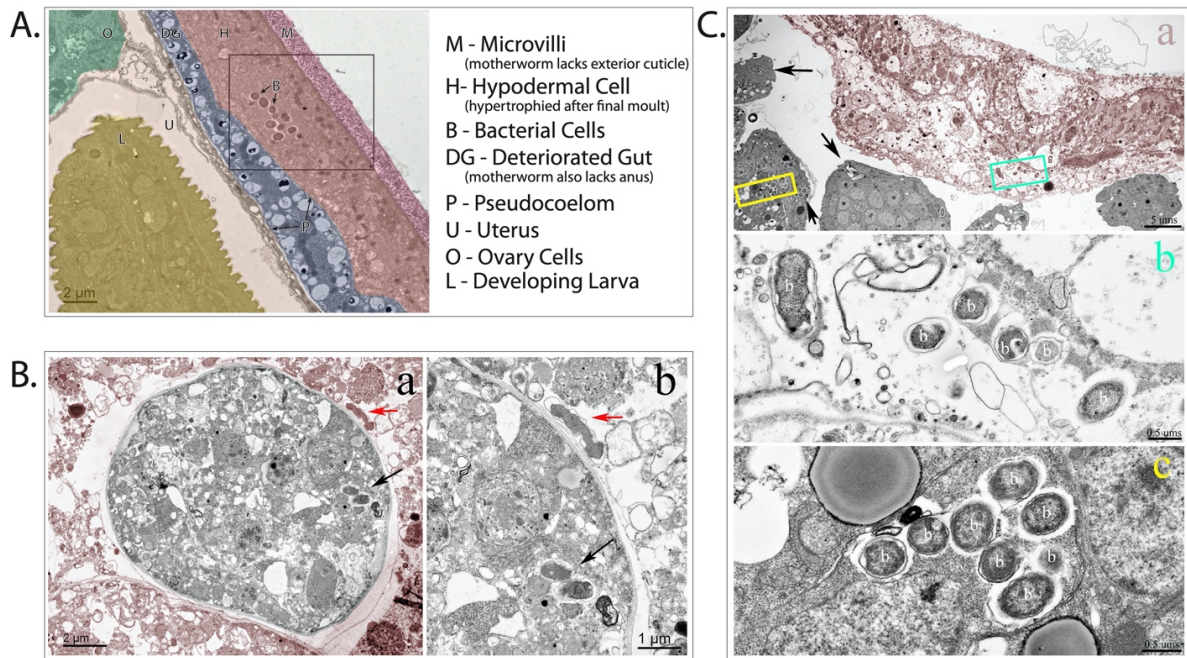


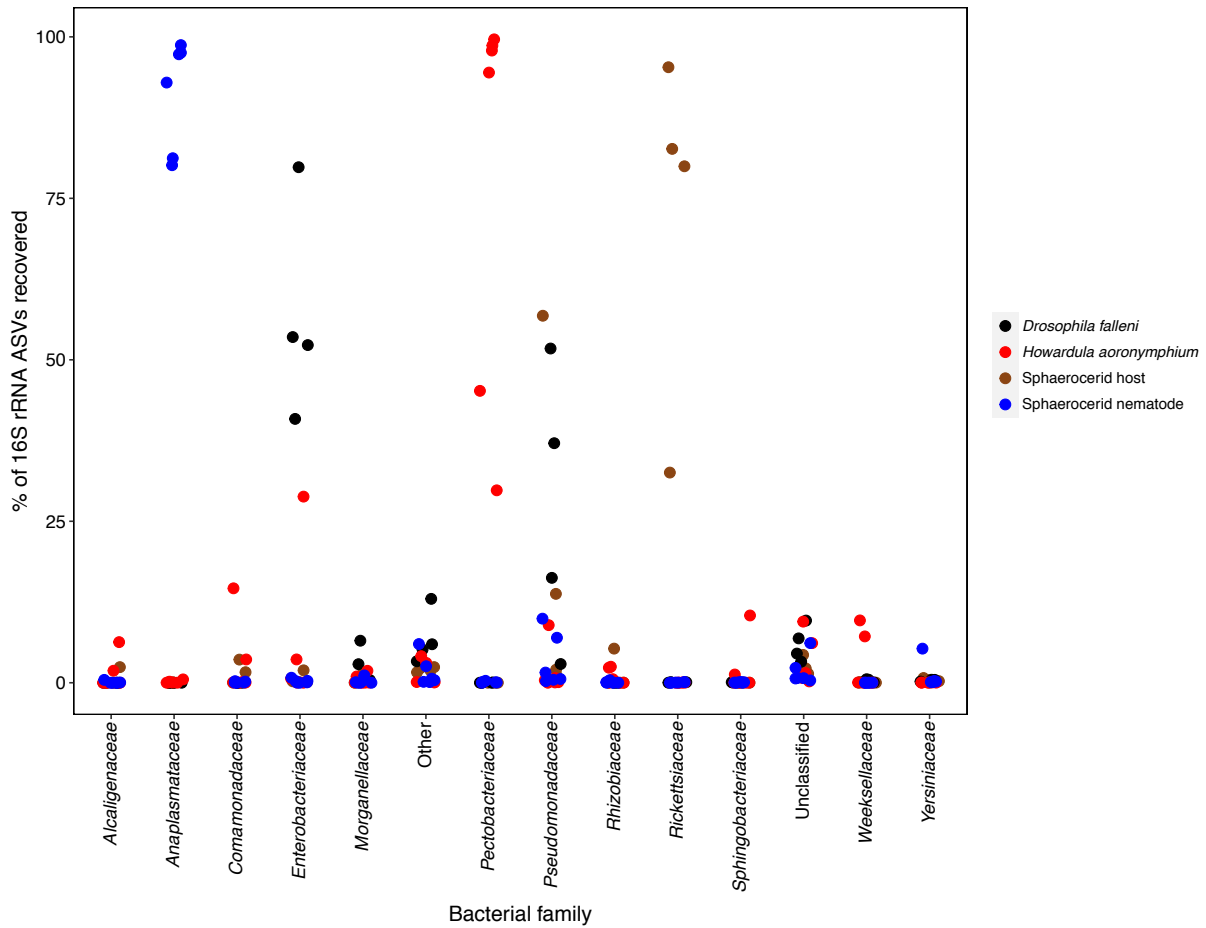
Figure S1. Tissue localization of bacteria within *Howardula aoronymphium* adults and juveniles.

Plate A. Localization of symbionts within a mother worm.

Plate B. Low magnification of sepia colored mother worm material with a grey scaled developing embryos/daughter worm within (a), higher magnification in (b) of the plate. The bacteria within the mother worm (red arrow for both figures) is external to the developing embryo/daughter worm. The bacteria within the developing embryo/daughter worm is shown by the black arrows.

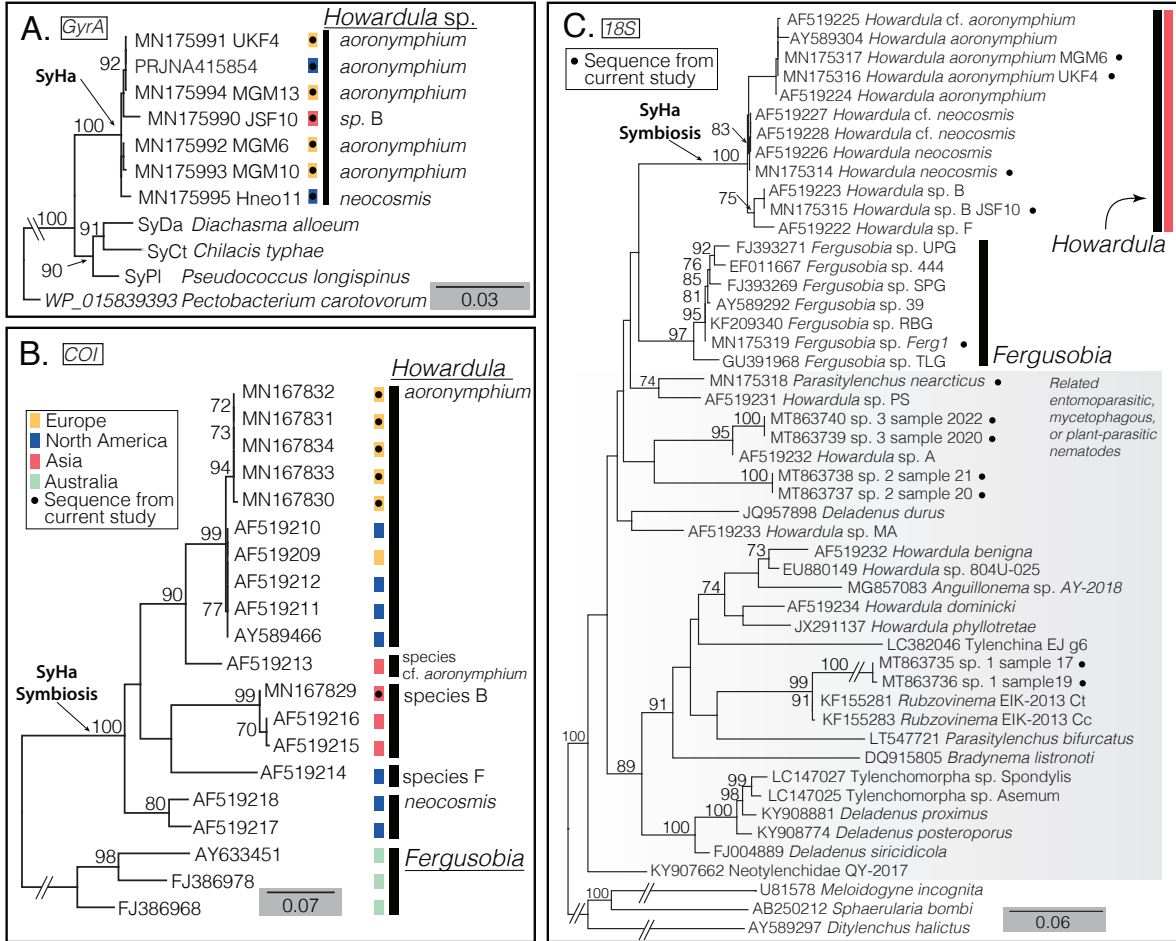
Plate C. Low magnification of a sepia colored mother worm cell wall and grey scaled developing embryos/daughter worms within the lumen of the mother worm (a). The teal colored box encloses bacteria within the mother worm and is the magnified in (b) of the plate (no longer sepia colored). The yellow colored box encloses bacteria within a developing embryo/daughter worm and is the magnified in (c) of the plate. The arrows within *figure a* show other groups of bacteria. The easily recognized bacteria in the magnified figures are labeled with a 'b'.

353
354
355
356
357
358
359
360
361
362
363
364
365
366
367
368
369



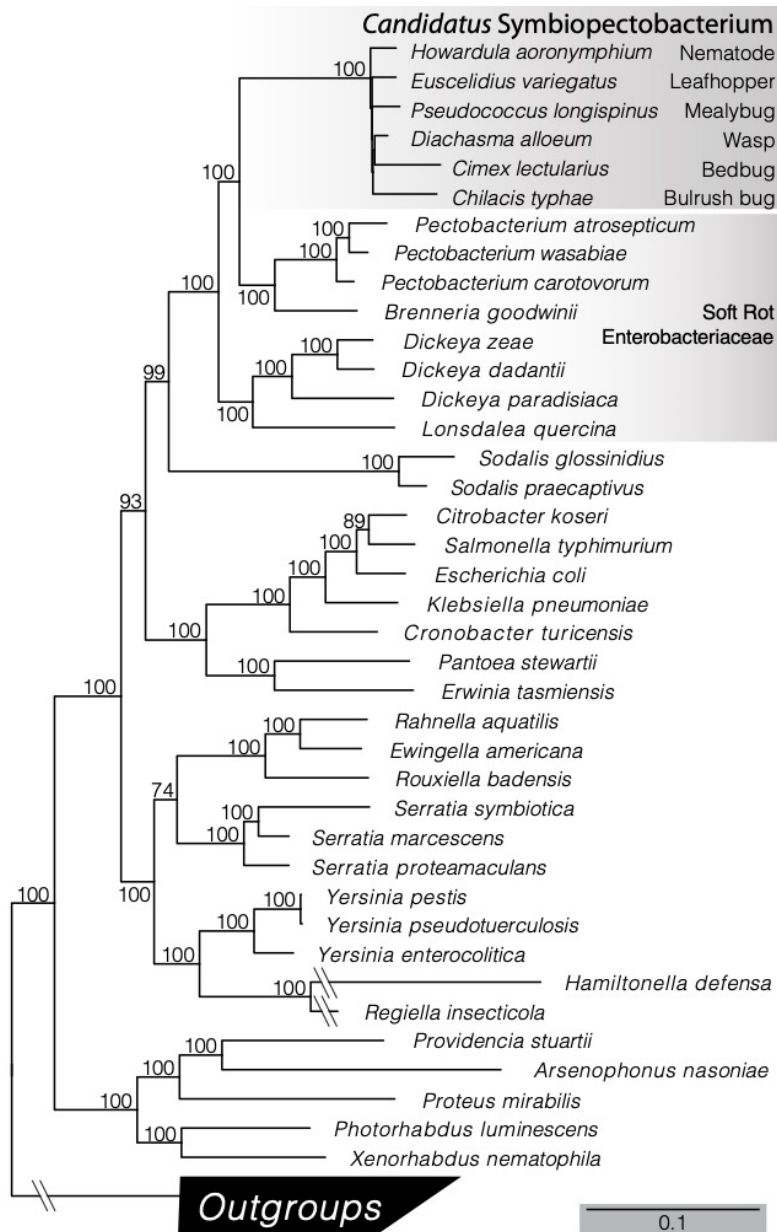
370
 371
 372
 373
 374
 375
 376
 377
 378
 379
 380
 381
 382

Figure S2. Relative abundance of V3V4 amplicon sequence variants according to bacterial family. The proportion of ASV counts corresponding to each bacterial family present across metagenomic datasets of *Drosophila falleni*, *Howardula aoronymphium*, *Spelobia* sp. (Sphaeroцерid host) and its nematode (Sphaeroцерid nematode species #3). ASVs that could not be resolved to the level of family are reported as unclassified. In order to avoid displaying excessive numbers of low-abundance bacterial families, we show only those that constitute > 5% of any individual sample. *Symbiopectobacterium* (=Pectobacteriaceae) is only present in *H. aoronymphium*, and is the only microbe found exclusively in all *H. aoronymphium* samples.



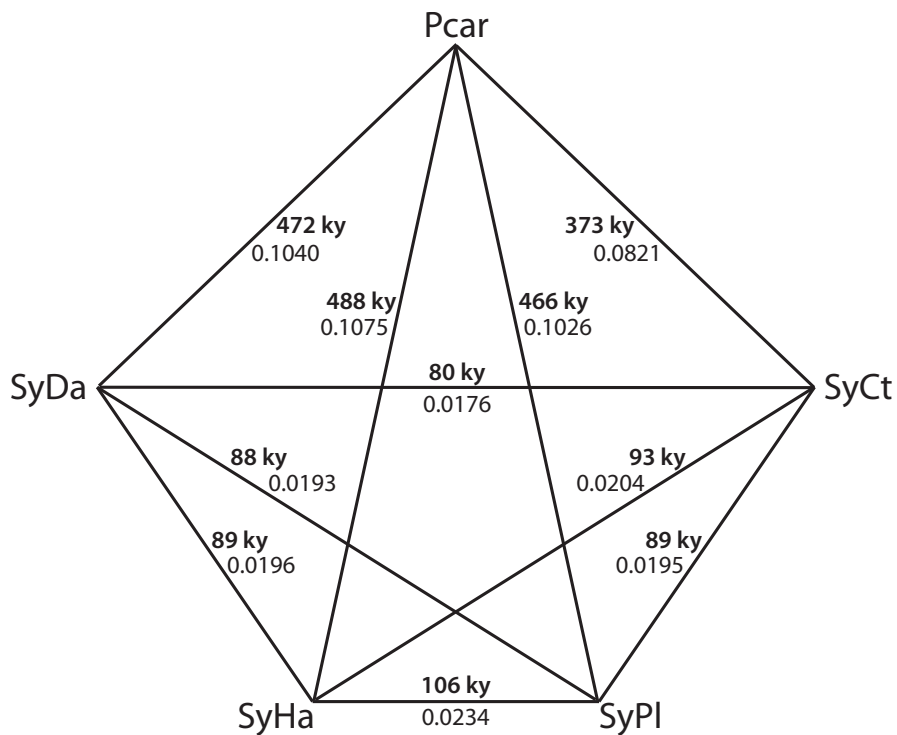
384
385
386
387
388
389

Figure S3. Phylogeny of *Symbiopectobacterium* using the gyrase A gene (*gyrA*) (A.). Phylogeny of nematode genes COI (B.) and 18S rRNA (C.). The *Howardula* clade harboring *Symbiopectobacterium* is highlighted with a red bar in the 18S rRNA phylogeny of nematode diversity (C). Sequences from the current study are marked with a black circle.



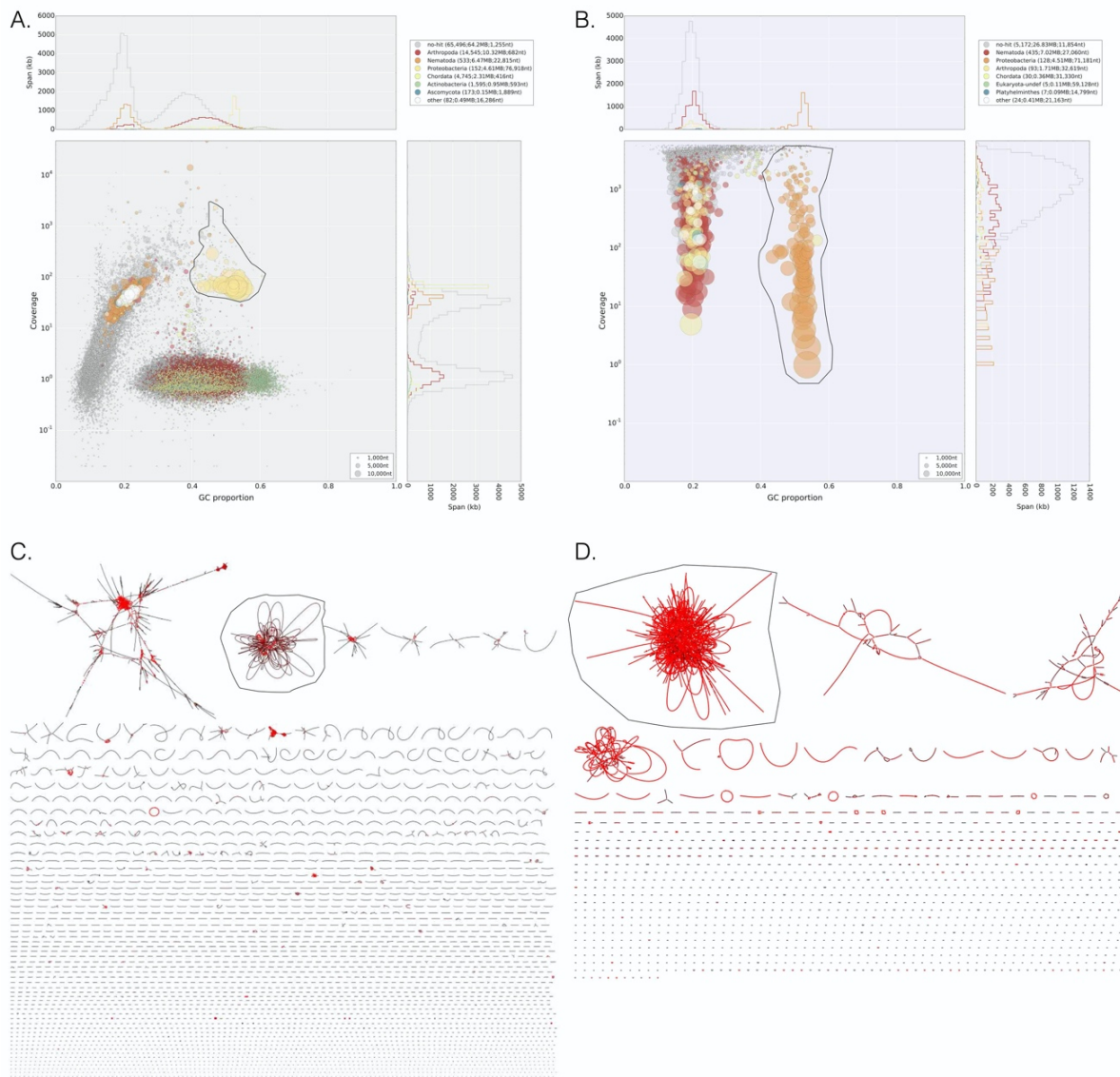
395
396
397
398
399

Figure S5. Phylogenetic tree of Gammaproteobacteria using the conserved set of 203 single copy orthologous genes. Phylogeny was constructed with RAXML using 100 bootstrap replicates.



400
 401
 402
 403
 404
 405
 406
 407
 408
 409

Figure S6. Divergence time estimates among *Symbiopectobacterium* species and their closest relative, *Pectobacterium carotovorum*. Substitution/site rate was calculated at the 2nd codon position for intact single copy ortholog (SiCO) genes (excluding pseudogenes). Divergence time was calculated using the measurement of 2.2×10^{-7} substitutions/site/year for the insect endosymbiont *Buchnera aphidicola* (28). Estimated divergence time (ky = thousand years) is in bold, substitution/site at 2nd codon position for intact genes is below. The number of SiCO genes used for comparisons differed for each pair (Pcar–SyCt 779; Pcar–SyPI 1692; Pcar–SyDa 1992; Pcar–SyHa 2001; SyCt–SyPI 707; SyCt–SyDa 754; SyCt–SyHa 741; SyPI–SyDa 1573; SyPI–SyHa 1786; SyDa–SyHa 1763).



410

411

412 **Figure S7.** Identifying the symbiont genome contigs within complex assemblies. A) Blobtools image of
 413 *Symbiopectobacterium* contigs among the *Howardula aoronymphium* A) metaSPAdes genome assembly and B) Unicycler.
 414 Visualization of the De Bruijn graphs for C) *Howardula* nematode symbiont (SyHa) and
 415 D) *Chilacis* bulrush bug symbiont (SyCt) constructed in Unicycler assembly showing links between
 416 contigs. Color indicates relative coverage of each contig (red = highest coverage).

417

418

Table S1. Primers and conditions for PCR and qPCR used in this project (42-48).

Primer reference	Target group	Target gene	Target length	Primer Name	Primer sequence (5'- to -3')	Cycling conditions
Folmer <i>et al.</i> 1994	<i>Drosophila</i> & sphaeroceids	<i>COI</i>	~700 bp	LC01490 HCO2198	GGTCAACCAATTCATAAAAGATATTGG TGAATTTTTTTGGTCACCCCTGAAGTTTA	
Jaenike & Brekke 2011	<i>Howardula</i>	<i>COI</i>	~300 bp	aoIF aoR	TTCGTTTTGGAGCTTTCAAAACCTGG AACACTTYGAAMCCAGATGAACCCAA	
Martinson <i>et al.</i> 2011 Sandström <i>et al.</i> 2001	Bacteria	<i>16S rRNA</i>	~1500 bp	27f-short 1507r	GAGTTTGATCCTGGGCTGA TAOCTTTGTTACGACTTCACCCCCAG	PCR -94°C for 2 min
Current study	<i>Ca. Symbiopectobacterium</i>	<i>purK</i> spacer	~1350 bp	n8_purK-p1498_F n8_purK-p1498_R	GTGACGCGGAGAACCATTTT GCTGTGAGGCTCTTCGTCCT	-35 cycles of 94°C for 30 s, 58°C for 30 s, 72°C for 90 s -72°C for 10 min
Current study	<i>Ca. Symbiopectobacterium</i>	<i>gyrA</i>	~1150 bp	SymbiopectogyrA_2f SymbiopectogyrA_2r	GTGACGCGGAGAACCATTTT GCTGTGAGGCTCTTCGTCCT	
Floyd 2005	<i>Howardula</i>	<i>18S rRNA</i>	~900 bp	Nem_18S_F Nem_18S_R	CGCGAATRGTCTCATTCACACAGC GGGGGTATCTGATGTCGC	
Current study	<i>Ca. Symbiopectobacterium</i>	<i>groEL</i>	158 bp	Symbiopecto_groEL_F Symbiopecto_groEL_R	CGGTGTGAAACGTTCTTCTGCTA ATGTCGATCATGTTGGCCGTA	PCR -94°C for 3 min -35 cycles of 94°C for 10 s, 55°C for 15 s, 72°C for 30 s -72°C for 5 min
Current study	<i>Ca. Symbiopectobacterium</i>	<i>16S rRNA</i>	1207 bp	Symbiopecto_16S_F Symbiopecto_16S_R	GAGCTTGCTCTCTGGGTTGAC TATGAGGATCCGCTTGGCTCTT	PCR -94°C for 3 min
Marchesi <i>et al.</i> 1998 Sandström <i>et al.</i> 2001	Bacteria	<i>16S rRNA</i>	1444 bp	63F 1507r	CAGGGCCTAACAGCATGCAAGTC TACCTTGTACGACTTCACCCCAAG	-35 cycles of 94°C for 30 s, 50°C for 30 s, 72°C for 90 s -72°C for 7 min
Current study	<i>Ca. Symbiopectobacterium</i>	<i>rplQ</i>	158 bp	Symbiopecto_rplQ_F Symbiopecto_rplQ_R	GTTTGTGAACCGGCTGATTACTCT TTCAGAAATGCGAGATATAACCAACC	qPCR Primer efficiency: 106.4%; r ² = 0.993
Ballinger <i>et al.</i> 2019	<i>Drosophila</i>	<i>rpl32</i>	161 bp	DrosFpl32-qF Drosrpl32-qR	CGCACCAAGCACTTCATCCG AGGGAGAGACGTACTCTGTTGT	qPCR

Table S2. Sequence information and collection source for members of *Symbipectobacterium* (29-41, 49).

GenBank Accession	Citation	Genome	Symbiosis Type	Host	Common name	Phylum	Order	Suborder	Superfamily	Notes
JQ013482	Unpublished	–	Facultative	<i>Koile paulula</i>	Leafhopper	Arthropoda	Hemiptera	Auchenorrhyn	Membracidae	
Z14096	Campbell <i>et al.</i> 1993	Degnan <i>et al.</i> 2011	Facultative	<i>Euseoides variegatus</i>	Leafhopper	Arthropoda	Hemiptera	Auchenorrhyn	Membracidae	Described as <i>Xyella</i>
EUJ27119	Duron <i>et al.</i> 2008	–	Facultative	<i>Cicadella viridis</i>	Green leafhopper	Arthropoda	Hemiptera	Auchenorrhyn	Membracidae	
MG93676	Issai-Kuh <i>et al.</i> 2017	–	Facultative	<i>Hyalesthes obsolus</i>	Planthopper	Arthropoda	Hemiptera	Auchenorrhyn	Membracidae	
AB772265	Koga <i>et al.</i> 2014	–	Facultative	<i>Aeneolamia conifera</i>	Froghopper	Arthropoda	Hemiptera	Auchenorrhyn	Fulgoroidea	Not mentioned in the publication.
AB772259	Koga <i>et al.</i> 2014	–	Facultative	<i>Aphrophora quadrinotata</i>	Spittlebug	Arthropoda	Hemiptera	Auchenorrhyn	Cercopodidae	Described as <i>Sodalis</i>
KF742539	Husnik & McCutcheon 2016	Husnik & McCutcheon 2016	Obligate	<i>Pseudococcus bryngisrus</i>	Long-bellied mealybug	Arthropoda	Hemiptera	Sternorrhyn	Coccidae	
DC418491	Unpublished	–	Facultative	<i>Erasoma lanigerum</i>	Wooly apple aphid	Arthropoda	Hemiptera	Sternorrhyn	Aphidoidea	
JQ726826-31	Matsura <i>et al.</i> 2012	–	Facultative	<i>Kielocorys resedae</i>	Birch catkin bug	Arthropoda	Hemiptera	Heteroptera	Lygaeoidea	
FF729479	Kuechler <i>et al.</i> 2012	This study	Obligate	<i>Chilacis typhae</i>	Burush bug	Arthropoda	Hemiptera	Heteroptera	Lygaeoidea	
HE586117	Kuechler <i>et al.</i> 2012	This study	Obligate	<i>Balonochilus numerus</i>	Sycamore seed bug	Arthropoda	Hemiptera	Heteroptera	Lygaeoidea	16S sequence has deletion
AB475157-140	Hosokawa <i>et al.</i> 2010	Bendt <i>et al.</i> 2016	Facultative	<i>Cimex lectularius</i>	Bed bug	Arthropoda	Hemiptera	Heteroptera	Cimicoidea	
JQ410807 sequence group	da Mota <i>et al.</i> 2012	–	Facultative	<i>Rhodnius</i> sp., <i>Dipetalogaster</i> sp.	Kissing bug	Arthropoda	Hemiptera	Heteroptera	Reduvioidae	
KX011894	Diaz <i>et al.</i> 2016	–	Facultative	<i>Rhodnius</i> sp., <i>Parstrongylus</i> sp.	Kissing bug	Arthropoda	Hemiptera	Heteroptera	Reduvioidae	
EUJ27118	Duron <i>et al.</i> 2008	–	Facultative	<i>Peris brassicae</i>	Cabbage butterfly	Arthropoda	Lepidoptera	Neolepidoptera	Papilionoidea	
KY124187	This study	Tvedte <i>et al.</i> 2019	Obligate	<i>Diachasma albeum</i>	Rhagoletis parasitoid wasp	Arthropoda	Hymenoptera	Apocrita	Sphaeruleroidea	
JQ046878	Salmonova <i>et al.</i> 2018	–	Facultative	<i>Howarthia acorinum</i> , <i>H. neocosmia</i> , <i>H. sp.</i>	Freshwater bryozoa	Bryozoa				
EF539551, EF178689, EF178670	Yashiro <i>et al.</i> 2012	–	?	<i>Pectratella magnifica</i>	Apple	Angiospermop	Rosales	Rosales	Angustelpodeae	
AB729551 sequence group	Pitman <i>et al.</i> 2008	–	?	<i>Plant, Solanum tuberosum</i>	Potato	Angiospermop	Solanales	Solanaceae	Solanoidae	Described as <i>Dickeya</i> .
	Someya <i>et al.</i> 2013	–	?	<i>Plant, Solanum tuberosum</i>	Potato	Angiospermop	Solanales	Solanaceae	Solanoidae	